Alexander

DELIVERABLE: D3.1

Development of innovative algorithms to identify congestion points in LV network

December 2022

UMONS Université de Mons · KU LEUVEN · ULB Université Libre de Bruxelles · Energy Ville · Universiteit Antwerpen · UHASSELT

elia · fluvius · ORES Opérateur des réseaux gaz & électricité · Sibelga energizing the city · resa

ALEXANDER PROJECT

ACCELERATING LOW VOLTAGE FLEXIBILITY PARTICIPATION IN A GRID SAFE MANNER

Deliverable D3.1

Development of innovative algorithms to identify congestion points in LV network

Author	Institution	E-mail
Hamada Almasalma	VITO	hamada.almasalma@vito.be
Lionel Delchambre	ULB	lionel.delchambre@ulb.be
Reinhilde D'hulst	VITO	reinhilde.dhulst@vito.be
Koen Vanthournout	VITO	koen.vanthournout@vito.be

Reviewer	Institution	E-mail
Helena Gerard	VITO	helena.gerard@vito.be
Patrick Hendrick	ULB	Patrick.Hendrick@ulb.be

This project has received funding from Energy Transition Fund 2021
FPS Economy, SMEs, Self-employed and Energy

Energietransitiefonds 2021
FOD Economie, K.M.O., Middenstand en Energie

December 2022

Executive Summary

This deliverable is developed in the context of the ALEXANDER project which aims to remove barriers that could block the full potential of the use of flexibility available in low voltage networks for the provision of system services. The deliverable presents the work of task 3.1 of work package 3.

Work package 3 aims to contribute to the unlock of flexibility by designing and implementing models and algorithms for active system management that allow cost-efficient flexibility procurement and activation in a grid-safe and coordinated way.

This deliverable contributes to the goal of work package 3 by designing a low voltage congestion forecaster. The forecaster identifies when and where congestions would arise in the distribution grid. The forecaster allows the formulation of grid constraints and provides spatially linked information on the risk for grid congestions to the stakeholders involved in providing system services. The algorithms and main innovations of the deliverable are summarized below:

- A low voltage congestion forecaster is designed to identify the risk for congestion in low voltage networks under flexibility activation. The main engine of the forecaster is a three-phase statistical Monte-Carlo based power flow.
- A novel method is designed to calculate the available headroom capacity on a distribution network asset. The proposed method is inspired by the geometric approaches to represent aggregated flexibility as a convex polytope.
- A flexibility model of a residential battery providing frequency containment reserve is designed and implemented. The model is used to study the impact of activating low voltage flexibility on low voltage grids.

This document describes the main objectives and innovations of the proposed models, as well as a brief overview of the algorithms. The academic IEEE low voltage test feeder is used in this deliverable as a case study to analyze the performance of the proposed methods. The results of the case study verify the ability of the proposed low voltage congestion forecaster to activate low voltage flexibility in a grid-safe manner.

Table of contents

List of Figures

Abbreviations

aFRR	Automatic Frequency Restoration Reserve
DSO	Distribution System operator
EV	Electric Vehicle
EU	European Union
FCR	Frequency Containment Reserve
FRR	Frequency Restoration Reserve
LV	Low Voltage
MV	Medium Voltage
OC	Overcurrent
OV	Overvoltage
PV	Photovoltaic
r	Maximum FCR capacity
RES	Renewable Energy Sources
SoC	State of Charge
TSO	Transmission System Operator
UV	Undervoltage
WP	Work Package

Chapter 1 Introduction

1.1 Context and motivation

The transition to the Belgian grid with high renewable energy resources (RES) is something we all want. RES are clean sources of energy that have a much lower environmental impact than conventional energy resources. The transition to RES will mitigate climate change by reducing greenhouse gas emissions, improve the environment and human health by decreasing air and water pollution, and support economic development [1].

Unfortunately, high penetration of RES comes with security of supply (adequacy) and system stability (balancing) issues. This is due to the high degree of fluctuation and low predictability of RES. Balancing and adequacy issues are serious problems that limit the increase of RES [2]. Hence, there is a need for innovative solutions and technology to solve these issues.

In the ALEXANDER project, we participate in letting the Belgian grid host more and more of RES without suffering from security of supply and stability issues. We do this by unlocking the flexibility of the low voltage (LV) consumers, and provide it as a service to support the grid. There is no doubt that LV flexibility will play an important role in supporting the Belgian grid.

1.2 Low voltage flexibility

Flexibility is the ability and will of a market participant to modify the production and/or consumption patterns, often in response to market incentives or price signals in order to provide a service to the system operator. As more and more intermittent and less predictable renewable generations are being connected to the grid, the grid operators require more flexibility to maintain the balance between supply and demand, and security of supply.

There is already a large potential for flexibility in LV networks. However, such potential is primarily theoretical and it is to be unlocked. Therefore, the main goal of the ALEXANDER project is to remove barriers that could block the full potential of the use of flexibility available in LV networks for the provision of system services [3].

1.3 Objectives and scope of WP3

Work package (WP) 3 consists of three tasks: 1) Task 3.1: development of algorithms to identify congestion, 2) Task 3.2: development of concept for flexibility provision from the LV grid and 3) Task 3.3: TSO-DSO coordination for activation and procurement of flexibility.

The three tasks of WP3 address the technical and operational barriers to the use of LV flexibility for the provision of system services. To safely activate the LV flexibility, grid constraints need to be calculated. If grid constraints become visible, grid operators may communicate and coordinate with the flexibility providers and flexibility markets to avoid grid congestion and safely activate flexibility.

Grid operators need a congestion forecaster to compute grid constraints. A congestion forecaster allows grid operators to identify where and when congestions will occur in the LV grid in case of activation of flexibility for system services (balancing), and provides spatially linked information on the risk for grid congestions to the stakeholders involved in providing system services. Congestion forecaster under flexibility activation is the main scope of task 3.1 and this deliverable.

Task 3.2 will focus on the dynamic express of the grid constraints and including them in the overall process of flexibility procurement and activation. The task will design different flexibility mechanisms (grid traffic lights) to make sure that grid constraints are not violated while activating the flexibility.

After selecting and implementing mechanisms to unlock LV flexibility, task 3.3 will focus on the day-to-day operational decisions as where and when flexibility needs to be applied, and how much flexibility is needed and at which cost. This decision making in daily operation is defined as the operationalization of flexibility and includes all the day-to-day operational decisions the system operators need to make in order to obtain the necessary flexibility. Task 3.3 will incorporate the findings of task 3.2 to design and examine possible market set-ups for Belgian-wide coordination between system operators for the procurement and activation of flexibility services.

1.4 The contribution of this deliverable

This deliverable presents the work of task 3.1 of WP 3. The deliverable presents the LV congestion forecaster (Figure 1-1) designed to identify the risk for congestion in LV networks (under flexibility activation) and to formulate grid constraints, based on a probabilistic state forecasting and in limited knowledge of loads, topology and electric characteristics.

The forecaster consists of four main blocks: 1) statistical load modelling, 2) statistical power flow, 3) congestion forecasting, and 4) calculation of grid constraints. The details of the forecaster are discussed in Chapter 2 with a case study on the calculation of risk for congestion.

The statistical load modelling is designed in such a way that can be easily expanded to include different flexibility models. In Chapter 3 of this deliverable, we focus on flexibility models of batteries providing frequency containment reserve (FCR). It is noteworthy that the statistical load modelling is designed in a generic way to incorporate different consumer preferences for flexibility activation. This will help to design a consumer-centric solution for the dynamic inclusion of grid constraints in the process of flexibility activation. The calculation of the grid constraints is detailed in Chapter 4. The interaction between the congestion forecaster and the energy markets (as shown in Figure 1-1) is not addressed in this deliverable. It will be addressed in task 3.3.

1.5 Outline

The reminder of this deliverable is organized as follows:

- Chapter 2 presents some literature review on congestion forecast, the LV congestion forecaster and a case study to show how the risk for congestion in LV networks can be calculated.
- Chapter 3 presents the flexibility model of a residential battery providing FCR and the impact of using flexibility to provide FCR on the grid. The work of this chapter is planned to be presented and published in IEEE PowerTech conference 2023.

- Chapter 4 proposes a novel method to calculate the available headroom capacity on a (distribution) network asset. The proposed method is inspired by the geometric approaches to represent aggregated flexibility as a convex polytope. The results of this chapter is planned to be published in a journal paper.
- The overall conclusion is presented in Chapter 5.

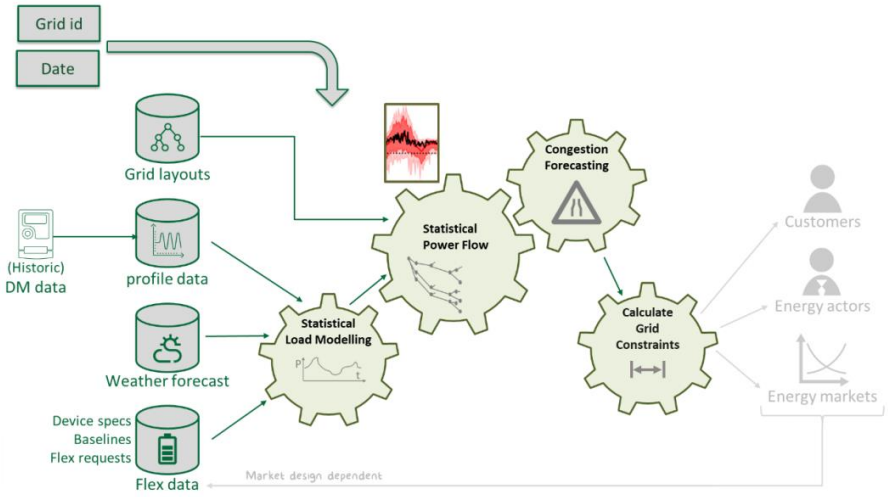

Figure 1-1: Schematic overview of the congestion forecaster

Chapter 2 LV Congestion Forecasting

2.1 Need

The report *Distribution System Operators observatory 2018 – Overview of the electricity distribution system in Europe* [4], published in 2019 by the JRC science for policy report emphasizes the new need for distribution system operators (DSOs) to develop congestion forecasting tools. This is necessary for the DSOs to predict the volumes of congestion occurring on their networks, to manage these local congestions and finally to fulfill their mission as network operator.

The article [5] points out that although the need for DSOs to access the congestion forecasting tool is increasing, the main commercial tools for advanced distribution management system (ADMS) do not explicitly provide congestion forecasting (e.g. the Network Manager ADMS provided by Hitachi Energy [6], the Spectrum Power ADMS provided by Siemens [7], the ADMS provided by Schneider electric [8]).

2.2 What is a congestion forecaster?

The report [4] briefly defines congestion forecasting tool as a combination of load forecaster and state estimation. Articles [5], [9] present a framework to forecast congestion built on the following blocks :

- Distribution grid data
- Probabilistic forecast of loads and generation
- Low voltage power flow
- Indices to assess congestion

2.2.1 Grid layouts

Several grid layouts can be used to forecast congestion, regarding the available data, as well as their quality. Article [10] reviews publicly available distribution datasets. It also characterizes (incl. methodologies, intentions, data origins, etc.) how grid datasets are compiled. Finally, it presents the following distribution network topology:

Grid typology	Use recommended by the articles
Synthetic grid	No real grid model, or obtained by simplifying/modifying a real mesh.
Example and test grid	Grid used for testing, validation or demonstration of a specific case.
Benchmark grid	Model used to compare the efficiency or validity of algorithms (more interest for the algorithm than for the grid).
Representative grid	Model capturing a specific network configuration, usually in an extreme case configuration.
Generic grid	Grid with parameters to vary grid representations. The difference with the representative grid is that for the representative grid, the parameters are

	fixed to capture the specificity of a grid, while for the generic grid, the parameters can be varied to represent different states of the grid.
Typical grid	Grid with averaged parameters, no extreme case.
Reference grid	Optimal grid regarding a specific criterion.

2.2.2 Probabilistic forecast of loads and generation

This section begins by reviewing the main literature reviews related to probabilistic and energy forecasting. It introduces the main reviews on the topic, then narrows the scope down to the LV load forecasting. Going through these reviews helps to get a good overview of the subject, as well as an idea of how research in LV load forecasting has evolved over the last few decades.

To start with, the article [11] reviews generally articles on energy forecasting, sorting articles according to their sub-areas (load, price, wind and solar) or forecasting methodology used (AI/ML, combined forecast and ensemble forecast, hierarchical forecasting, probabilistic forecasting). A bibliometric analysis is applied to 22 journals, focusing on the journals publishing the most energy forecasting articles. The journal with the highest number of load forecasting publications is International Journal of Forecasting. The review also provides links to open databases used for energy forecasting. Finally, the review provides advices to improve the quality of the article (e.g. need to use a reproducible data set, ensure the correct use of evaluation metrics, need to use correct terminology, compare results with state-of-the-art methods, etc.).

The review [12] stresses the need to use probabilistic load forecasts for the distribution network due to the following criteria: little data available, high load volatility due to low demand aggregation, large number of different load profiles. [13] completes this list of arguments by stating that new storage technologies will disrupt conventional load profiles and that the probabilistic forecasting tool is suitable to handle these issues. Therefore, this deliverable focuses on probabilistic models.

In a general perspective, article [14] reviews the state-of-the-art of probabilistic forecasting, considering the main theories, methodologies and main applications (e.g. inflation rate, temperature, precipitation accumulation) in the mid-2010s. The review does not focus on energy load forecasting, but provides the basics for understanding general forecasting techniques.

More specifically on probabilistic power flows, [15] reviews articles studying probabilistic power flows based on the two following techniques: numerical approach and analytical approach. It also presents specific cases considering nonlinear equations, change of network configuration, interdependence of stochastic variables. Finally, it gives an overview of possible applications such as electrical system planning, voltage control, decentralized generations integration, three-phase imbalances and harmonic studies.

Article [16] provides literature review on probabilistic load forecasting considering techniques (meaning group of models such as Multiple Linear Regression, or Artificial Neural Networks (ANN)), methodologies and evaluation methods. It firstly sorts articles according the methodology used (short-term load forecasting time horizon from less than one day to two weeks, and long-term load forecasting from two weeks to more than three years) or the application (probabilistic load flow, unit commitment, reliability planning, other). Nevertheless, methods considered are mainly for the transmission grid.

Focusing more on the LV side, article [17] provides a review of the literature on residential electricity consumption and applications of smart meter data. It differentiates the residential load forecast between top-down models using global variables (demographics, national statistics) and bottom-up models inferring global consumption by studying household consumption. Bottom-up approaches are divided into: conditional demand analysis, ANN, physical models, and probabilistic models. About forecasts, the article reviews sources of information, modeling techniques as well as performance measures. It also lists the available low voltage profile datasets.

Still from the point of view of smart meters, the article [13] provides a literature review on smart meter applications. It presents several ways to develop forecast using a smart meter (e.g. traditional method, deep learning, clustering, aggregation), or not (e.g. demand response, weather modeling and selection, forecasting hierarchical). It then presents how probabilistic forecasting can be derived from classical point forecasting by generating multiple generations of scenarios, using a probabilistic forecasting model (e.g. regression quantile) or post-processing point forecasts. The article insists on the need to better understand the impact of storage systems on the load forecast at the LV level.

Finally, the article [12] reviews 221 articles related to LV load forecasting. It begins by presenting the main differences between LV loads and medium voltage (MV)/high voltage (HV) loads. It then presents main methods, some available LV datasets, main applications (design/planning, operation, trading and simulation of inputs) and challenges encountered in forecasting LV loads. It recommends moving towards a probabilistic load forecast given the significant load variability along the seasonality. It highlights the interest of studying the evaluation of the peak forecast at the LV side.

2.2.3 Low voltage power flow

The article [18] presents the specificities of distribution load flows: radial structure, high R/X ratio, multi-phase and unbalanced operations or distributed loads and decentralized generation. For these reasons, the generic Newton Raphson algorithm used to solve power flow problems on the transmission network could turn out to be irrelevant. The algorithms to solve the power must therefore intrinsically consider the low voltage specificities.

Even though consideration of the proper power flow algorithm is necessary, the problem is not challenging today. Indeed, it is well known because it has been studied for decades, with for example the article [19] published in 1967.

2.2.4 Indices to assess congestion

The results of the previous probabilistic power flow must now be interpreted to assess congestion. The definition of congestion is essential to obtain relevant results. This section is built in three blocks presenting:

- Formal definitions of congestion in the European regulation
- Congestion indices used in the literature
- EU standards and norms
- Local DSO practices

i. Formal definition of Congestion in the EU regulation

According to the REGULATION (EU) 2015 /1222 [20], congestion is defined as:

- 'Market congestion' means a situation in which the economic surplus for single day-ahead or intraday coupling has been limited by cross-zonal capacity or allocation constraint;
- 'Physical congestion' means any network situation where forecasted or realized power flows violate the thermal limits of the elements of the grid and voltage stability, or the angle stability limits of the power system;

The REGULATION (EU) 2019/943 [21] of the European Parliament and the Council of 5 June 2019 on the internal market for electricity defines congestion as:

- 'congestion' means a situation in which all requests from market participants to trade between network areas cannot be accommodated because they would significantly affect the physical flows on network elements which cannot accommodate those flows;
- structural congestion' means congestion in the transmission system that is capable of being unambiguously defined, is predictable, is geographically stable over time, and frequently reoccurs under normal electricity system conditions.

ii. Congestion indices used in the literature

Article [5] uses three indicators to assess congestion through their color map tool:

- Node voltage – voltage at a node and deviation from nominal value (threshold: 1.03 p.u.)
- Branch load - ratio of a branch's load to its nominal current (threshold: 0.5 p.u.)
- Transformer load – ratio of transformer load to rated capacity (threshold: 0.3 p.u.)

Article [9] uses the three following indicators to asses congestion:

- Nodes voltage deviations – Deviation of the node voltages compared to specified value (critical node: more than 3% deviation for 20% of simulations)
- Branch overloading – Ratio of branch's current to rated thermal capacity (critical branch: branch overloading 100% for 20% of simulations)
- Transformers overloading – Ratio of transformer power to rated capacity (critical transformer overloading: transformer overloading 100% for 20% of simulations)

2.3 Overview of the congestion forecaster used in the ALEXANDER project

2.3.1 Description of the forecaster

The schematic overview of the congestion forecaster architecture is shown in Figure 1-1. The LV congestion forecaster; used in the ALEXANDER project; aims at calculating the risks for congestion on LV distribution feeders for a forecasted day. The tool addresses four types of congestion: undervoltage, overvoltage, overcurrent and overloading of the MV/LV transformers. The congestion risks are defined as the probability a particular congestion may take place and is based on a predefined risk threshold that is calculated per node and per time step.

The congestion forecaster does not deterministically calculate congestions, as for this calculation the necessary input would be impossible to acquire (e.g. deterministic forecasts of load profiles are not

available), but merely outputs a congestion risk based on the statistically possible LV feeder state during the forecasted period.

The calculations within the congestion forecaster are based on historical, and (if available) daily grid and connection profile measurements, as well as weather forecasts. The tool assumes that the grid layout is known, however the phase-connectivity of the single-phase connections is assumed to be unknown by the DSOs.

Next to the congestion risks, the forecaster also calculates the so-called 'headroom' per network asset, i.e. the maximum available capacity on the respective feeders and MV/LV transformer that can be activated in worst case without causing any congestion on the feeder/transformer. The details of the headroom calculations are addressed in Chapter 4.

2.3.2 Input data

The following inputs are required by the congestion forecaster:

- A list of IDs of the assets (feeders and MV/LV transformers) for which a congestion forecast should be calculated.
- The LV grid layout data, including meta-specs on the connections.
- A representative set of historical digital meter measurements, including meta-specs on the measured connections.
- If available, daily meter measurements from all smart meters in the feeders and grids under consideration
- Exogenous data: historic weather data and weather forecast, comprising at least of temperature, cloud coverage and solar irradiance.
- Transformer measurements on the feeders/transformers considered (if available).
- Measurement on the measured switch locations in the feeders considered (if available).
- Forecast of the voltage on the MV/LV transformer (if available). If not available 230V/400V is assumed.

2.3.3 Algorithms and main innovations

The LV congestion forecaster comprises the following:

- A Monte-Carlo based statistical three-phase power flow is used to forecast the range and probabilities of voltages and currents per grid node and per quarter hour (96 values for the next day).
- Based on a predefined risk threshold, the risk for overcurrent, overvoltage, undervoltage and transformer overloading is calculated from the probabilities and range of the forecasted voltages and currents within grid.
- The power inputs to the power flow are sampled from historical profiles, since deterministic power offtake/injection forecasts are unavailable. The sampling makes use of weather forecasts for increased accuracy.
- Grid layout data is assumed to be known, phase-connectivity of single-phase connections is also sampled, as this phase connectivity remains unknown.

- The congestion risk assessment includes a worst-case model of the flexibility. This model assumes flexible assets are on at full power, all the time. If more data on flexible asset use is available to the DSO, this model can be made less coarse.
- Compared to state of the art, this congestion forecaster does not rely on any measurement (digital meter or other), to make a reliable, yet robust, estimation of the risks for congestion in a known LV network. A set of representative historical profiles are the only requirement to make this statistical assessment.

2.4 Case study

2.4.1 Grid and load data

Figure 2-1 shows the IEEE European Low Voltage Test Feeder used in this deliverable to study the different implementations proposed. The given LV network test bench is available with the time series data for 55 single phase loads. More details about the feeder and its load profiles can be found in [22], [23].

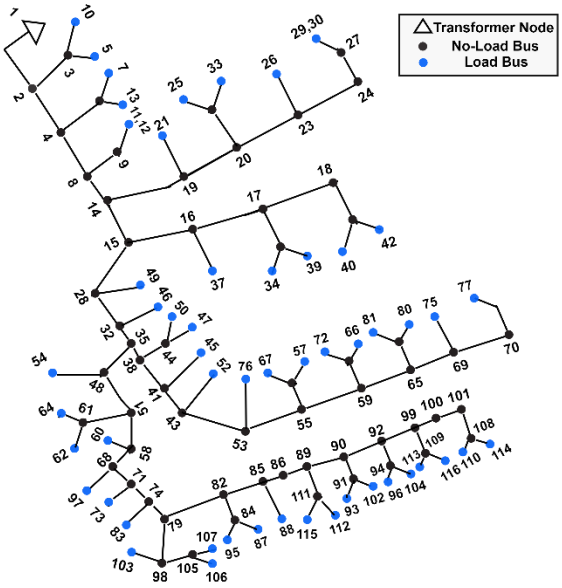

Figure 2-1: IEEE EU LV Test Feeder (based on [23])

2.4.2 Congestion forecast

The LV congestion forecaster was tested on the IEEE LV Test Feeder. 15-minute time step was considered in the statistical power flow (96 time steps per day). One daily load profile has been assigned to each customer based on the load profiles detailed in [22], [23]. The assigned load profile of each customer was considered as the average load profile. The Monte-Carlo engine of the statistical power flow was set to 100 scenarios. 100 load profiles for each customer were sampled based on the average load profile and a defined standard deviation. The standard deviation of each customer was set to half of the average active power.

The undervoltage congestion is defined as the voltage below 0.95 pu. The overvoltage congestion is defined as the voltage above 1.05 pu. The current congestion is defined as the current higher than the 100 A.

Figure 2-2 shows voltage profiles of the three phases of node 114 (at the end of the feeder where most voltage problems are expected to occur). One can clearly notice that voltages of the 100 scenarios are within the defined limits 1 ± 0.05 pu. Therefore, it is not expected to have voltage congestion.

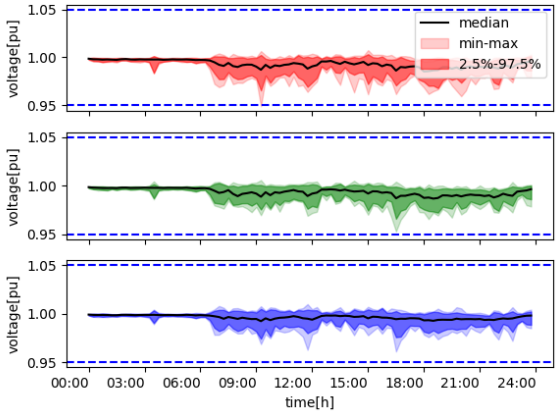

Figure 2-2 Voltage profiles of bus 114

Figure 2-3 shows current profiles of the first branch after the transformer, the one between nodes 1 and 2. As shown in the figure, the current in few scenarios goes above the rated current. Hence, It is not expected to have current congestion.

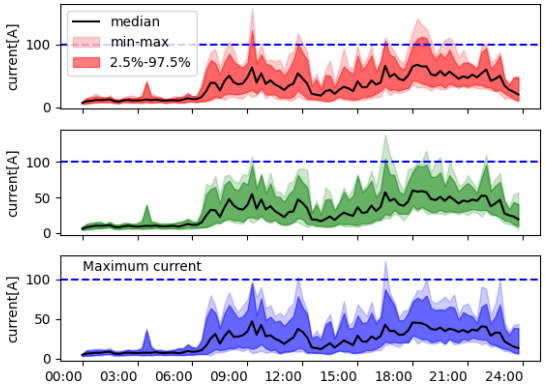

Figure 2-3 Current profiles of the branch between nodes 1 and 2

An overview of the calculated congestion risk is shown in Figure 2-4. As expected from the previous analysis and confirmed by the congestion risk analysis, it is very unlikely to have a congestion.

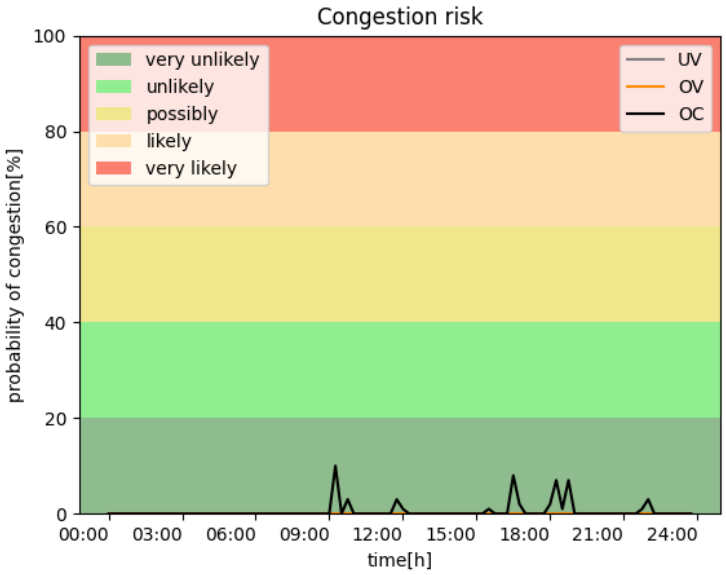

Figure 2-4 Calculated congestion risk. UV: undervoltage, OV: overvoltage, OC: overcurrent

The average daily load profiles of the IEEE feeder have been scaled by 1.5 factor, for more validation of the LV congestion forecaster. Voltage profiles of node 114 are shown in Figure 2-5. Majority of voltage profiles of the 100 scenarios are within the voltage limits. Therefore, voltage congestion probability is expected to be low in this case.

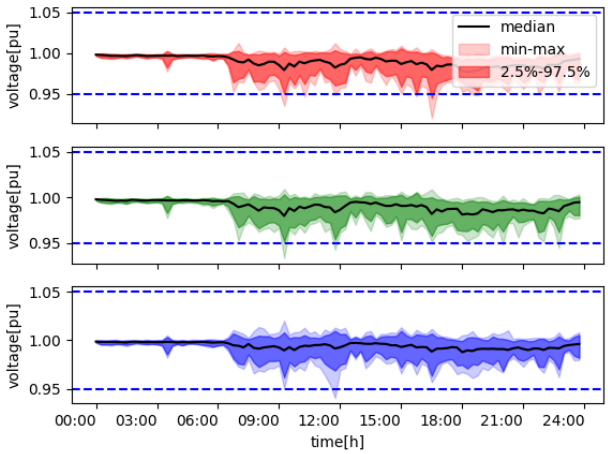

Figure 2-5 Voltage profiles of bus 114 (scaled case)

Figure 2-6 shows the current profiles of the branch between nodes 1 and 2. Some of the current profiles in this case cross the 100 A limited. Hence, it is possible in this case to have a current congestion.

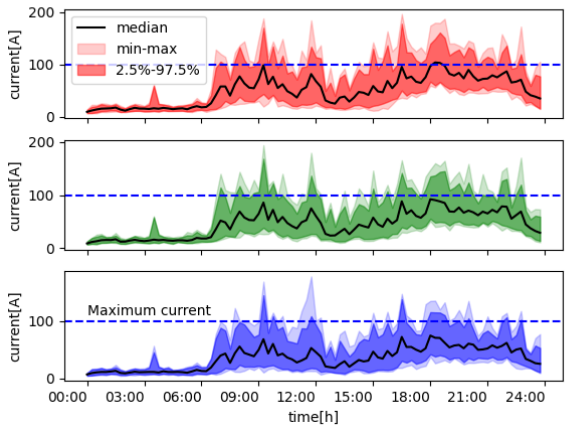

Figure 2-6 Current profiles of the branch between nodes 1 and 2 (scaled case)

The calculated congestion risk of the scaled case study is shown in Figure 2-7. The congestion risk calculation indicates that the current congestion is possible and the overvoltage/undervoltage congestions are very unlikely. One can notice that the congestion risk calculation agrees with the previous analysis.

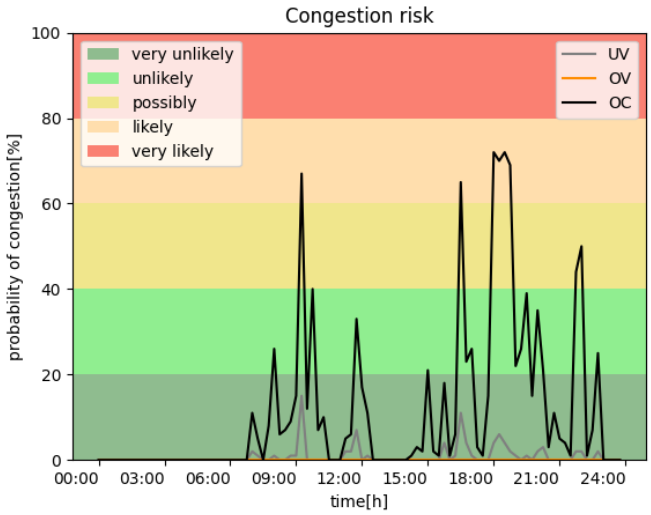

Figure 2-7 Calculated congestion risk (scaled). UV: undervoltage, OV: overvoltage, OC: overcurrent

Chapter 3 Probabilistic assessment of LV grid congestion caused by flexibility assets providing FCR

3.1 Introduction

3.1.1 Causes leading to changes in the distribution network

Distribution electrical grids are expected to change in the next few years, impacted by the following causes:

- Political targets to achieve the goals of the Paris Agreements and ensure a sustainable world for future generations [24], [25].
- New European regulatory framework empowering new stakeholders (e.g. active prosumers, energy communities, etc.) and enabling new activities (e.g. energy sharing, self-consumption, flexibility for DSOs, etc.) [21], [26], [27].
- Decentralization of production and storage because power plants are multiplying and decentralizing with the deployment of renewable energy generators (hydraulic, wind, photovoltaic panels, etc.), and electricity storage solutions are also called upon to decentralize [28].
- Technological advances leading to several impacts:
    - From the point of view of consumption, new ways of using electricity with the arrival of electric vehicles, heat pumps, new local storage devices which lead to a local increase in electricity consumption [29]–[31].
    - On the monitoring side, digitization, smart meters and the availability of much more detailed data increase the potential for flexibility [32].
- Change in customer behavior made possible by the new regulatory framework and the growing awareness of climate challenges and new technologies, end users can access more information and better control their energy. They thus can become active players in the market. A change in behavior can also be observed given the rise in energy prices at the end of 2021 [30].

3.1.2 Distribution end-users towards more flexibility

The previously mentioned changes to the electrical distribution grid will lead to an increase in possible congestion. Indeed, production and consumption will increase, be more volatile and less predictable.

In this context, the Clean Energy Package offers a new framework for redesigning the electricity market with new players and new activities. In addition, it encourages DSOs to integrate the flexibility potential of Distributed Energies [28]. Regulation (EU) 2019/944 [21] and Directive (EU) No 2019/944 on the Internal Electricity Market Design [27] allow DSOs access to tools and flexibility services to manage the expected increase in congestion.

Similar increase in production and consumption volatility and a decrease in predictability are also expected from the transmission perspective. In addition, the increase in renewable energy will lead to a reduction in inertia. In this context, TSOs will have to increase their flexible services to preserve security of supply. They will therefore increasingly rely on flexible sources and services, such as those newly available at the distribution level. By activating or deactivating flexible distribution assets to provide

frequency ancillary services, they can cause congestion at the distribution level, increasing congestion risks for DSOs [30].

The new regulatory framework is therefore an opportunity for DSOs to better manage congestion, and conversely a risk when TSOs use flexible distribution assets. This brief introduction highlights the need to study the impact of low voltage flexible assets providing frequency ancillary services on the distribution network.

3.1.3 Related work

Energy storage systems are good candidates for providing services to the grid [33]. Among storage systems, low-voltage assets such as residential batteries are increasingly studied to provide grid services [37], such as:

- Peak shaving - [34] presents an optimization problem for residential batteries to provide peak shaving and promote PV penetration into the LV grid. [35] presents a LV energy storage system control strategy for peak shaving and voltage control. [36] performs an optimization problem to mitigate overvoltage and overcurrent while reducing battery degradation.
- Frequency ancillary services - [38] optimizes the combination of residential batteries providing frequency reserves with self-consumption and [39] studies economy benefits of combining self-consumption with frequency restoration reserve (FRR). [40] considers the problem from the aggregator point of view who wishes to optimize a pool of flexible LV assets providing FCR, given the Belgian regulatory constraints.

Nevertheless, few articles consider the impact caused by these LV flexible assets on the low voltage grid. [42] studies the LV grid congestion caused by LV aggregate loads providing frequency regulation in North America. The article focuses on transient responses, considering the characteristics of protection systems for congestion constraints. [41] studies the congestion on a European LV network caused by batteries providing self-consumption combined with other activities, such as frequency reserves. However, the paper uses deterministic power flow to measure the impact, without capturing the uncertainty of grid loads.

3.2 Problem statement

The problem introduced in the last section is therefore stated as: "What is the impact of flexible assets on LV grid congestion?". Two parts require clarifications and are deepened above:

1. How to characterize the flexible assets?
2. How to define congestion constraints?

3.2.1 Residential batteries providing FCR as flexible assets

This sub-section presents the justification to choose residential batteries providing FCR as flexible assets.

Frequency ancillary services – Several frequency ancillary services currently exist [21]:

- FCR - Provides frequency containment reserves from prosumer flexibility (R1) - is open to demand-side participation, aggregation and independent aggregation. Resources connected to the distribution grid are theoretically allowed to participate but, in practice, the process is quite complex and involves DSO verification.

- Automatic FRR (aFRR) - Provides automatic frequency restauration reserves from prosumer flexibility (R2) - is expected to open to demand-side response (with independent aggregation still limited to Active Customers with certain types of contracts).
- Manual FRR – Provides manual frequency restauration reserves from prosumer flexibility (R3) - is open to demand-side response (and independent aggregation) participation. This product can be offered through an availability contract and/or free bids.
- RR - Provides frequency replacement reserves from prosumer flexibility (slow R3).

We decide to focus first on the FCRs because they are the fastest reserves to activate and are needed to be studied to reduce network frequency volatility. Indeed, production of renewable energy should increase leading to a relative reduction in the inertia of synchronous generators. This means that faster frequency control reserves will be needed in the near future.

Nevertheless, other frequency ancillary services must be considered and be modeled afterwards as to their relevance. For example, aFRR is expected to have a greater impact on LV congestion because of higher requested volumes of energy and higher time of activation than for FCR.

FCR mechanism – Flexible assets participating in FCR provide an output power proportional to the deviation of the grid frequency from the nominal frequency (50Hz). The maximum power is activated when the frequency deviation reaches a predefined maximum value (200 mHz in continental Europe) and within 30 seconds in continental Europe. The output power profile of a flexible assets participating in FCR is presented in Figure 3-1.

If the batteries fail to deliver the pre-contracted power output, the asset provider will face steep fines. It is therefore important to ensure that the electrical capacity is available for the contractual period and therefore to control the state of charge.

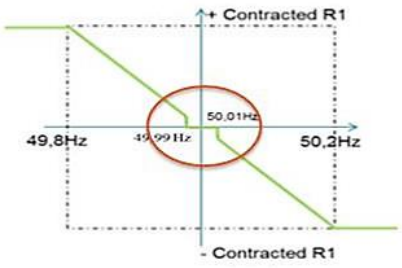

Figure 3-1: FCR output power profile[33]

Technologies – WP2 of the Alexander project identifies the following LV technologies capable of providing flexibility: heat pumps, water boiler with storage, PV, residential batteries and electric vehicles.

Among these technologies, we decide initially to focus on residential batteries because it is a simple model to start with and is a good candidate to fast frequency control reserves due to their fast response time. In addition, the main purpose of residential batteries is to store electricity, while other flexible devices have other purposes: heat pumps and water heaters with storage aim to provide heat, the PV initially aims to generate electricity and electric vehicles are mainly used for mobility purposes. These other technologies will be modeled afterwards considering their specificities.

3.3 Methodology

This section presents the methodology used to model the batteries following the FCR and the impact analysis on the LV grid.

3.3.1 Batteries following FCR model

Flexible batteries are modeled as constant power following a frequency deviation as long as energy is available in the battery over a given safety range. The model receives a frequency signal as an input, and provide a power profile as output, as showed in the Figure 3-2.

Figure 3-2: Battery model providing FCR services input and output

Frequency signals considered are either (i) historic signal or (ii) worst-case signal. A safe range represented by a percentage of the state of charge (SoC) is required and used as a parameter because batteries such as lithium-ion batteries cannot be used below or above a specific threshold to ensure safe use of the battery. It also allows for a more accurate model because the open current voltage (OCV) may not realistically be considered constant for a low or high SoC. In this configuration, OCV is considered constant, i.e. SoC is independent, as showed in the Figure 3-3.

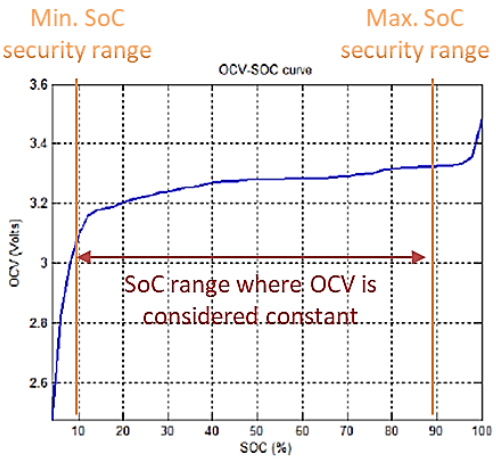

Figure 3-3: Experimental OCV-SoC curve showing min./max. settings. SoC and Parameterized SoC where OCV is considered constant

The choices of frequency signals selection, battery models and power output are presented below.

Frequency signal – Two frequency signals are considered for the FCR: (i) a historic signal with high frequency deviation (January 8, 2021) and (ii) worst-case scenarios.

(i) The historic frequency signal is provided on Elia's website. Regarding volumes of data, public data is only provided since June 2022. A request was sent to access data from the specific day of January 8, 2021 when the frequency deviation is expected to be particularly high due to the worst imbalance event on the European network since two last years. The data is provided on a granularity of 10 seconds and 4 features are provided: datetime, actual frequency, FCR contracted by Elia (kWh volume) and FCR actually requested (kWh volume).

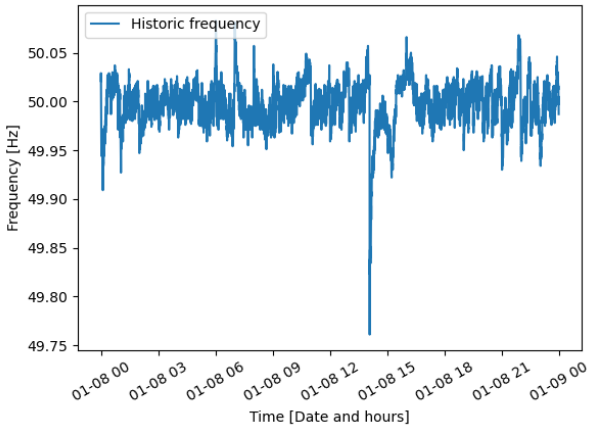

Figure 3-4: 10 seconds historic frequency signal – January 8, 2021

(ii) The worst-case scenarios are defined based on the Elia FCR design note art. 4.5.1. defining FCR requirements for flexible assets with a limited reservoir such as residential batteries. The article states that "[…] This might mean in the worst case scenario a combined requirement of 30 minutes (first constraint for alert state situation) and 10 minutes (equivalent energy constraint for the worst case scenario of "normal mode" operation), namely 40 minutes" [44]. This recommendation is based on Article 156 of EC Regulation 2017/1485 [26]. This means that the worst-case scenario for the FCR is that the flexible assets are activated at full power for 40 minutes. To be more precise, there are two worst case scenarios, one where the batteries are considered to consume at full power (e.g. -10kW) and the other where batteries are considered to inject at full power (e.g. +10 kW). Congestion indices are assessed per 15 minutes and available energy is not considered.

FCR – As explained in the definition of the FCR service, power output of flexible assets providing FCR should be proportional to the frequency deviation. This can be modeled by the following equations:

$$P_{bat}^{k} = r\Delta f^{k}$$

$$\Delta f^{k} \begin{cases} \dfrac{f_{nom} - f^{k}}{\Delta f_{max}} & if\ \Delta f_{db} < |f^{k} - f_{nom}| < \Delta f_{max} \\ -1 & if\ f^{k} - f_{nom} \geq \Delta f_{max} \\ 1 & if\ f^{k} - f_{nom} \leq -\Delta f_{max} \\ 0 & \text{otherwise} \end{cases}$$

Where:

- k is the 10 second time step of the frequency signal
- Δf_{max} is the frequency deviation for which maximum power contracted r is activated (200mHz for continental Europe)
- f_{nom} is the nominal frequency of the grid (50Hz for continental Europe)
- Δf_{db} is the frequency deadband over which no power should be injected or consumed (10mHz in continental Europe)

Battery models - literature identifies three main battery models:

1. White box model – A set of partial differential equations are needed to describe the physical and chemical phenomena inside the battery (e.g. ion diffusion phenomena, reaction kinetics, mass and charge balance, temperature effects). These models present a high precision but also a complex model structures with a low-speed operation. It is also possible that analytical solutions do not exist, and parameter identification is challenging. There are separated in two sub-models: electrochemistry model, that was then completed by specific mathematical model.
    - Electrochemistry model –There are three domains: a negative electrode, a positive electrode and a separator. The model must be discretized in x and r directions, resulting in several states equations. [45] , [46]
    - Mathematical modelling of a battery – based on one of the electrochemical modelling, empirical equations or math-based stochastic models are used in mathematical models. It evaluates the charge of recovery effect and ignore other factors.
2. Grey box mode – The battery is considered an open circuit voltage source connected to electrical components. The model estimates battery voltages based on current inputs and different resistor-capacitor branches. Grey box models are discriminated into 5 subclasses [45], [47], [46]:
    - Simple models - the battery is modeled as an ideal voltage source coupled to an internal resistance. Simple models do not consider charge/discharge rates, SoC, and other nonlinear effects.
    - Thevenin based models - this model is more accurate than simple models because it can provide transient responses using more RC loops. This model typically offers the ability to capture two time-dependent effects: depletion and recovery. The SoC can be determined using the Coulomb counting procedure or a more complex method such as an extended Kalman filter. Circuit parameters are obtained using an HPPC (Hybrid Pulse Power Characterization) test. Accurate parameter estimation is difficult due to nonlinear effects. Comparison between battery model and experimental response of the battery is necessary to validate the model.
    - Impedance-based models – For example, War Burg's impedance model. In these models, the parameters are defined on the method of Electrochemical Impedance Spectroscopy (EIS). Each component of the circuit represents an electrochemical process. The components cannot therefore be approached by RC elements. Converting these models from frequency domain to time domain could be complex. It can also be difficult to match battery transient characteristics and models operating only at fixed SoC values.
    - Runtime-based models - use coupled power networks and tables to define SoC, battery runtime, cell voltage, and thermal characteristics. They accurately simulate battery life, voltage during direct current discharge process. Nevertheless, these models are not good in case of variable current discharges (due to low accuracy during transient characteristics of the battery). These models are complex and inaccurate in predicting battery characteristics.

- Combined models – The last subclass considers all combinations of battery sub-models presented previously.

3. Black box model - Articles [47], [46] also complete this list of models with the black box models. The main idea is to estimate battery parameters with data-driven approaches such as fuzzy-based estimation, fuzzy-based neural network, artificial neural network, bio-algorithm inspired, the support vector machine, etc.

The impact analysis; in this deliverable; considers the balance of production and consumption on a quarter-hourly basis. Therefore, the transient response is not needed and a simple gray box model can be used to represent the output power of the batteries while comparing the complexity and expansiveness of the models.

The output power is therefore proportional to the frequency deviation as long as energy is available in the battery, r is considered as a constant. Indeed, batteries are flexible assets with a limited reservoir. In that context, not only power output, but also available energy in the battery should be considered

Figure 3-5 shows one 10kW/10kWh battery model following FCR:

- Historic frequency is the 10 second frequency signal of January 8, 2021.
- The battery power output shows the power injected (>0) or consumed (<0) on a 10-second basis, following the frequency deviation.
- The battery available energy represents the energy available in the battery.

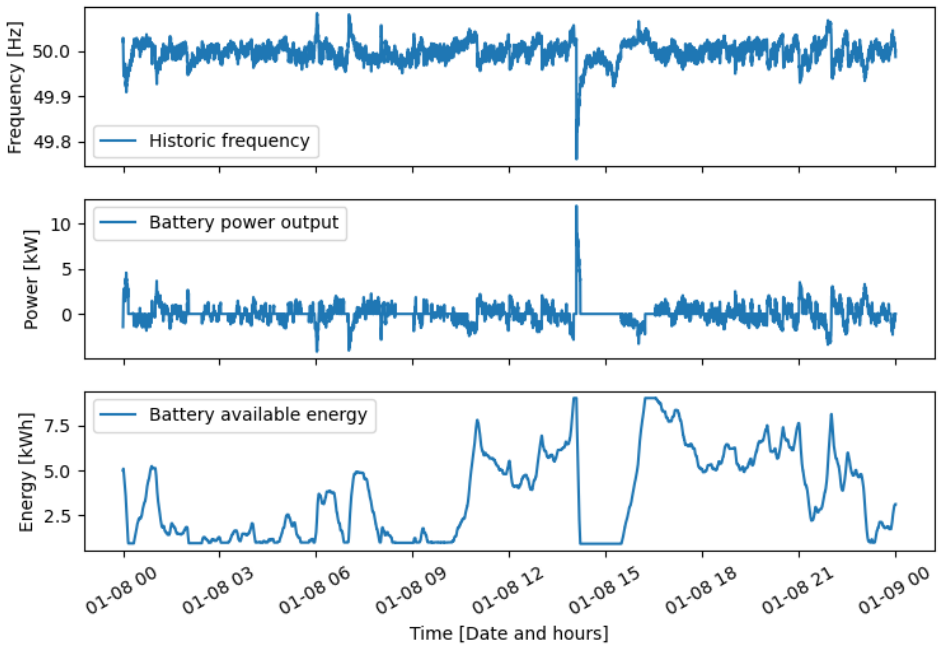

Figure 3-5: Historic frequency with battery output power and available energy – January 8, 2021

The figure shows that when frequency is over 50.01Hz, the battery will consume electricity from the grid and the available energy will increase. Conversely, when the frequency is below 49.99, the battery will inject electricity on the grid and the available energy will decrease. It is also visible that around 2:30 p.m., the timing on which the incident historically occurred on the European network, the frequency dropped

below 49.8 Hz. The battery therefore provides maximum power as long as the energy is available. When there is no more energy in the battery, the battery stops injecting electricity.

3.3.2 Impact analysis

The impact analysis is carried out by computing a probabilistic assessment of the residential batteries distributed on a LV network. The probabilistic character of the calculation is based on the spatial position of the batteries on the network and not on the battery power output signal which is deterministic.

To be more precise, a scenario is first defined with a fixed quantity of batteries with parametrized power and energy to be distributed (for example: scenario 1 with 5 batteries, scenario 2 with 10 batteries, scenario 3 with 15 batteries, etc.). Then, for each scenario, the batteries are normally distributed a certain number of occurrences via the Monte Carlo engine described in Chapter 2Chapter 2 (for example 200 occurrences). Figure 3-6 shows one occurrence where batteries are normally distributed on the LV grid for a scenario with 4 batteries [10kW/10kWh]. In this study, batteries are considered to be used 100% for FCR.

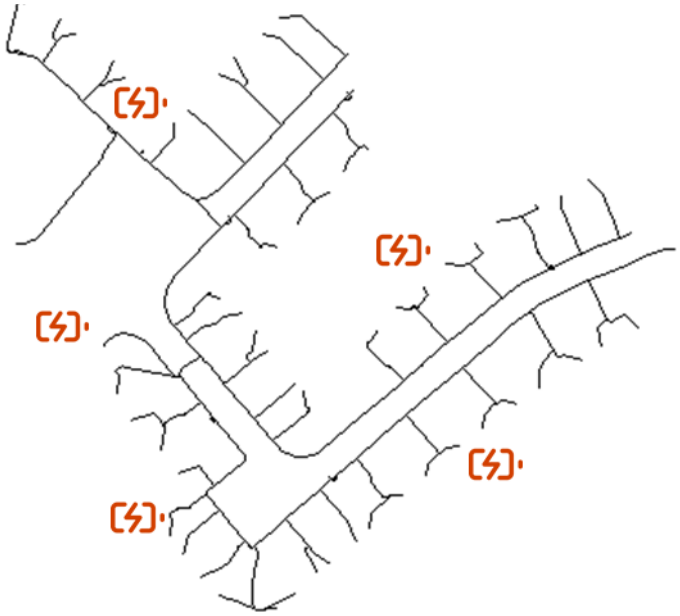

Figure 3-6: One occurrence of batteries normally distributed on the IEEE EU LV test feeder for a scenario with 5 batteries [10kW/10kWh]

For the impact analysis, power outputs are resampled from 10 seconds to 15 minutes. To be more realistic, average power is used to compute thermal limits and maximum power is used to compute voltage limits. Indeed, overcurrent must be considered over a given period because components heating presents a thermal inertia. Conversely, voltage protection (such as the voltage controller on inverters) are activated directly when an overvoltage or undervoltage occurs, to protect devices. Then, power flows are computed for each occurrence, for each scenario and for each 15-minutes time steps over a specific day (e.g. January 8, 21 for historic data).

Some probabilistic frequency signals were calculated based on a standard deviation around 50 Hz. But this probabilistic signal did not seem realistic, and the study of the features influencing the evolution of the frequency signal for the next months/years seems to fall out of the scope of the Alexander project. Moreover, the historical signal already shows interesting results on the injection/consumption of synchronized batteries distributed on the grid, and the worst-case scenario gives information (maximum

impact of batteries following FCR) on the future impact of decentralized flexible assets providing frequency ancillary services on the low voltage network.

For the LV network, the simplified IEEE EU LV test feeder [48] is considered, as explained in Chapter 2. The results of the previous probabilistic power flow must now be interpreted to assess congestion. The definition of congestion thresholds is necessary to define whether the network is congested or not. Congestion indices are presented in Chapter 2. In this study, following thresholds are used:

- Overvoltage (OV) – Occurrence of a 10-second voltage signal exceeding 1.05 p.u.
- Undervoltage (UV) – Occurrence of a 10 second voltage signal going below 0.95
- Overcurrent (OC) – Current signal exceeding 200 A ampacity for power averaged over a period of 15 minutes

3.4 Results

The following results are presented to highlight congestion probability occurring on the LV grid caused by distributed residential batteries providing FCR signals:

- Probability of congestion occurring for UV, OV and OC over a day (15-minutes period), considering the entire LV network.
- Probabilistic voltage and current over a day for each phase, for one specific branch or specific bus.
- Probabilistic voltage over a day and for all busses, represented as a heatmap.

3.4.1 Probabilistic congestion risk

Figure 3-7 and Figure 3-8 show the risk of UV, OV and OC occurring over a period of one day. The risk is identified on all buses (UV and OV) and all branches (OC) of the LV network. Figure 3-7 presents the results for 10 batteries following historic frequency signal distributed on the low voltage grid and Figure 3-8 presents the results for 40 batteries. Each scenario is studied for 200 configurations.

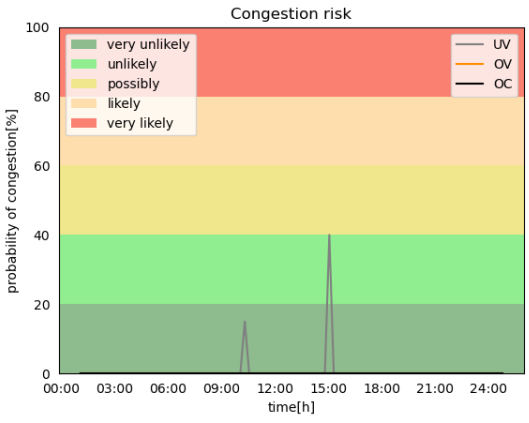

Figure 3-7: Congestion risk for 10 batteries following historic frequency signals

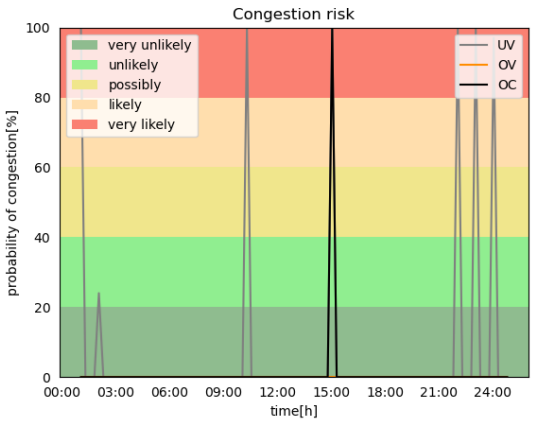

Figure 3-8: Congestion risk for 40 batteries following historic frequency signals

These figures show that undervoltage is more likely to occur than overcurrent with fewer batteries distributed across the grid. This comes from the used historical signal: the maximum power is reached but for a short time (a few minutes). Voltage limits are instantaneously reached, but current limits have

inertia and are therefore not reached because the period is not long enough to exceed the congestion limits.

3.4.2 Probabilistic voltage and current over a day for each phase, for one specific branch or specific bus

The following figures show the voltage on the bus 114 when 10 batteries are randomly distributed on the low voltage grid for one day and for each phase. Figure 3-9 shows voltage when batteries are following the historic signal and when considering end-users are not consuming any electricity. Figure 3-10 shows voltage when batteries are following the historic signal and when considering LV consumption profiles provided by the IEEE EU LV test feeder. Figure 3-11 shows voltage when batteries are following a worst-case signal (consuming maximum power) and when considering LV consumption profiles provided by the simplified IEEE EU LV test feeder.

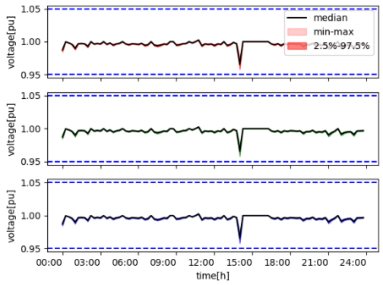

Figure 3-9: Voltage on bus 114 with historic frequency and no residential profiles

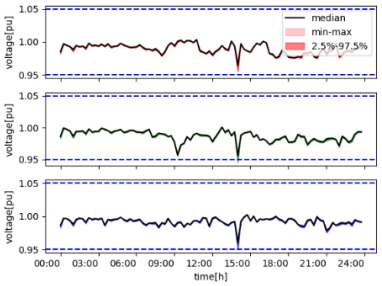

Figure 3-10: Voltage on bus 114 with historic frequency and residential profiles

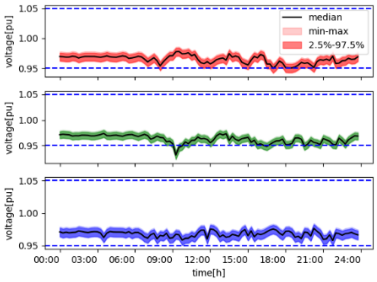

Figure 3-11: Voltage on bus 114 with worst-case frequency residential

The following figures show the current on the branch 0 when 10 batteries are randomly distributed on the LV grid for one day and for each phase. Figure 3-12 shows current when batteries are following the historic signal and when considering end-users are not consuming any electricity. Figure 3-13 shows current when batteries are following the historic signal and when considering LV consumption profiles provided by the IEEE EU LV test feeder. Figure 3-14 shows current when batteries are following a worst-case signal (consuming maximum power) and when considering low voltage consumption profiles provided by the IEEE EU LV test feeder.

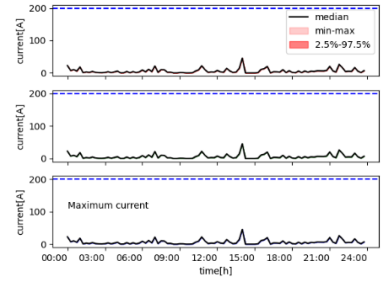

Figure 3-12: Current on branch 0 with historic frequency and no residential profiles

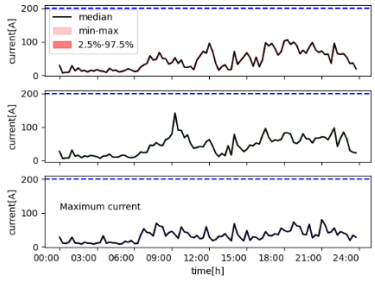

Figure 3-13: Current on branch 0 with historic frequency and residential profiles

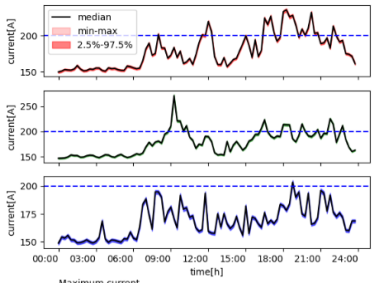

Figure 3-14: Current on branch 0 with worst-case frequency and residential profiles

3.4.3 Probabilistic voltage over a day and for all busses, represented as a heatmap

The following heatmap shows the undervoltage on all the busses when 10 batteries are randomly distributed on the LV grid for one day and for each phase. Figure 3-15 shows voltage when batteries are following the historic signal and when considering end-users are not consuming any electricity. Figure 3-16 shows voltage when batteries are following the historic signal and when considering LV consumption profiles. Figure 3-17 shows voltage when batteries are following a worst-case signal (consuming maximum power) and when considering low voltage consumption.

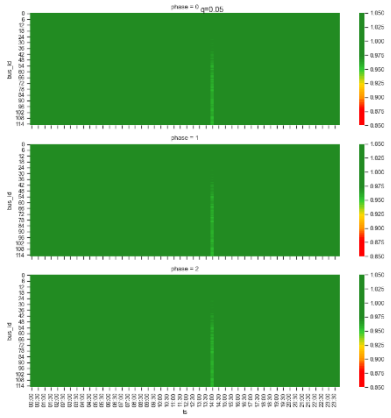

Figure 3-15: Voltage on all busses with historic frequency and no residential profiles

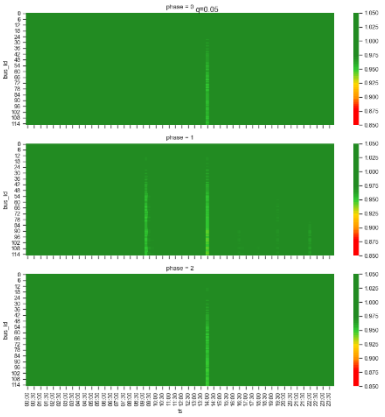

Figure 3-16: Voltage on all busses with historic frequency and residential profiles

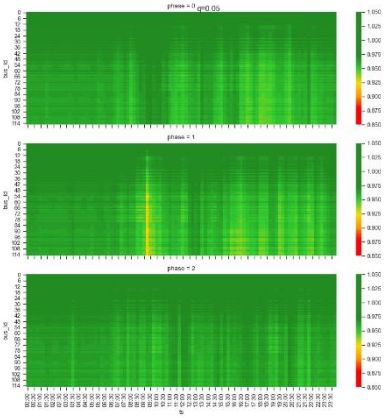

Figure 3-17: Voltage on all busses with worst-case frequency and residential profiles

3.4.4 Summary table

Table 1 summarizes results for the following cases:

- Scenarios – 10 scenarios are considered, from 0 to 45 batteries randomly distributed on the grid with a 5-batteries step
- LV consumption profiles – End-users with and without LV consumption profiles are considered
- Frequency signal – Three frequency signals: the historic frequency signal of January 8, 21 and with two worst-case scenarios (maximum power consumed and maximum power injected)
- Congestion – Three congestion constraints are considered: UV, OV and OC.

For each case, 200 battery configurations are tested and for each configuration, the power flows are performed 96 times (a whole day with 15-minute time steps). The table summarizes the results of 1,152,000 power flow runs.

Table 1: Summary table of impacts caused by batteries providing FCR

[No: no congestion occurrence probability, VU: very unlikely that congestion occurs (less than 20% probability) U: unlikely that congestion occurs (between 20% and 40% probability), P: possibility that congestion occurs (between 40% and 60% probability), L: likely that congestion occurs (between 60% and 80% probability), VL: very likely that congestion occurs (more than 80% probability)]

		Without low voltage end-users									**With low voltage end-user**								
		Historic			**Worst-case (consuming max power)**			**Worst-case (injecting max power)**			**Historic**			**Worst-case (consuming max power)**			**Worst-case (injecting max power)**		
		UV	**OV**	**OC**	**UV**	**OV**	**OC**	**UV**	**OV**	**OC**	**UV**	**OV**	**OC**	**UV**	**OV**	**OC**	**UV**	**OV**	**OC**
scenarios (number of batteries distributed on the grid)	**0**	No	No	No	No	No	No	No	No	No	No	No	No	No	No	No	No	No	No
	5	No	No	No	No	No	No	No	No	No	No	No	No	VU	No	VL	No	No	No
	10	VU	No	No	No	No	No	No	No	No	P	No	No	VL	No	VL	No	No	No
	15	VL	No	No	U	No	No	No	VU	VL	VL	No	No	VL	No	VL	No	P	VU
	20	VL	No	No	VL	No	VL	No	VL	VL	VL	No	No	VL	No	VL	No	VL	VL
	25	VL	No	No	VL	No	VL	No	VL	VL	VL	No	No	VL	No	VL	No	VL	VL
	30	VL	No	No	VL	No	VL	No	VL	VL	VL	No	No	VL	No	VL	No	VL	VL
	35	VL	No	No	VL	No	VL	No	VL	VL	VL	No	No	VL	No	VL	No	VL	VL
	40	VL	No	No	VL	No	VL	No	VL	VL	VL	No	VL	VL	No	VL	No	VL	VL
	45	VL	No	VL	VL	No	VL	No	VL	VL	VL	No	VL	VL	No	VL	No	VL	VL

Chapter 4 LV feeder headroom capacity: a geometric approach.

4.1 Introduction

4.1.1 Flexibility within the European market context

It has been clear for quite some time now that in order to reduce carbon emissions to a level where the global temperature does not rise above 1.5°C, an acceleration of the installation rate of renewable energy resources (RES) will be required [49]. Additionally, electrification of transport, through electric vehicles (EVs), and heating, using heat pumps, will be crucial. It is also clear that flexibility will be key to ensure a secure and reliable power supply, e.g. to cope with the variability and uncertainty that renewable energy often brings. Many of the new RES installations will be connected to the low voltage (LV) distribution network, just as EV chargers and heat pumps for residential use. Also, electricity end-consumers are becoming crucial players due to their potential to provide the necessary flexibility by adapting their consumption behavior.

The Distribution System Operators (DSOs), managing and operating the LV distribution grids, have to make sure that their existing (LV) networks are capable of hosting a maximal amount of renewable energy sources, and that new types and more loads can be integrated. Yet, at the same time, the flexibility provided by the end consumers creates unpredictable and coordinated power flows in the distribution networks.

Within the unbundled energy system in Europe, DSOs hold a natural monopoly on (distribution) network management. An independent regulator oversees their activities [50]. Current policy limits the role of DSOs as *neutral market facilitators*, leaving competitive activities to the market [51] .

Aggregators are often the intermediary party responsible for taking the combined flexibility from different resources to the market, for instance, as a frequency response service. These markets are typically suited to global objectives but lack the granularity required by the DSO to solve their local problems. On the other hand, the coordinated activation of resources concentrated in weak spots of the distribution network might result in local congestions.

The fact is that the aggregators are not necessarily aware of certain network constraints, and do not have the necessary information at hand to evaluate these congestion risks. DSOs generally do not share their grid data nor do aggregators in general have an idea of the non-flexible offtake/injection profiles on the same network. The DSOs, in their role of neutral market facilitator, must provide the necessary flexibility activation constraints to the market to make sure that their network does not get into a congested state when a certain flexibility is selected. This often results in strict pre-qualification requirements or a conditional access of flexible resources to the flexibility market, as e.g. the system used in Belgium [52].

A new set of flexibility activation constraints is proposed here. It is reasonable to assume a reporting obligation towards the DSO for resources employed in flexibility services. Given that information, the DSO can provide to the flexibility market a simplified representation of the maximal available capacity on their feeders and MV/LV transformers for simultaneous activation of any flexibility resources. We

refer to this maximal available and allowed flexibility as the available *headroom* on a certain network asset.

In network segments with enough spare capacity and few flexibility resources, the DSO might conclude that the devices can be activated simultaneously to their maximum capacity without causing any issues. This is the case where a simple pre-qualification procedure suffices.

In a situation with a larger number of flexibility resources, the DSO might limit their simultaneous activation by communicating the available *headroom*. This is a region that delimits the allowed power consumption/injection range for the activation of flexible resources on a network segment. Even though the effect of flexibility activation in the distribution grid is location-dependent, the headroom region *does not discriminate against the activation of specific resources*, a legal principle that is often put in place.

Inside the headroom region, the aggregator is free to decide which flexibility resources will be activated or not. The headroom calculation generates constraints that are relatively simple and can be taken into account in the aggregator bidding or the market clearing process. A setup where the headroom constraints are included in the market clearing is illustrated in Figure 4-1.

This avoids the complexities of sharing detailed network information and the operational points of each particular feeder, which are time-dependent and influenced by the non-controlled loads. Including the headroom not only ensures a secure operation of the network but also makes sure that more flexibility resources can participate in the market.

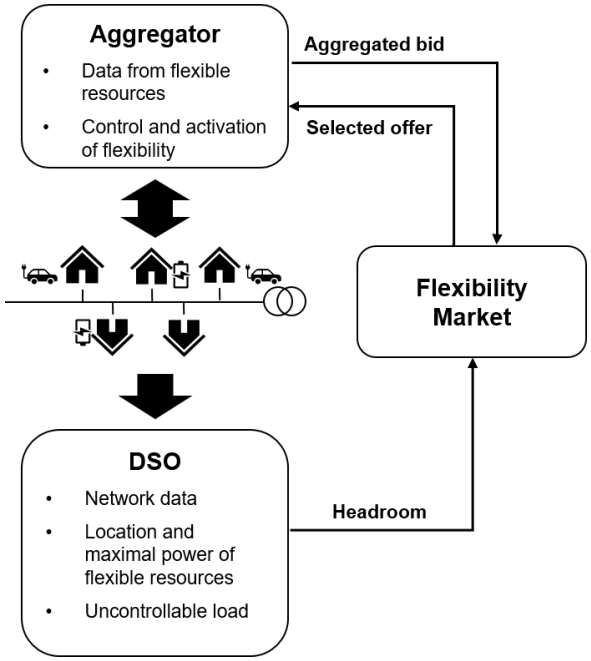

Figure 4-1: Schematic illustration of the flexibility market setup: the DSO only provides the headroom to the flexibility market, the aggregator is in charge of managing and controlling the flexible resources

4.1.2 Related work

Many approaches have been proposed to characterize or approximate resource aggregated flexibility, to be included in its aggregated form in an ancillary market [53]–[56]. Often in these works, the objective is to build an aggregated model composed of flexible resources that can be activated without violating user comfort or operational constraints. This aggregated form can be included in (multi-period) optimization problems, such as the ancillary services market clearing or unit commitment optimization [57], [58].

Some recent papers use methods derived from geometric theory to concisely model large collections of loads [59]–[61]. In these works, flexible loads are modeled as convex polytopes, defined as the bounded, feasible sets delimited by their linear constraints. The aggregation of these polytopes can be seen as their set-wise sum known as the Minkowski sum.

Computing the exact Minkowski sum is intractable for a large number of polytopes, but inner and outer approximations of the Minkowski sum can be found in polynomial time, as e.g. done in [54], [55]. This provides the aggregators with a tractable characterization of their load portfolio.

Some works include network constraints as additional constraints in the aggregation step and/or in the optimization of the flexible resources [62]–[64]. Others already start with a definition of flexibility consistent with network constraints, as in [65].

These approaches frequently assume that the DSO, or an agent that has access to all the information, is able to optimize and control flexible resources respecting network constraints. This cannot be easily applied in the current market framework, and, as explained above, it is not always allowed by regulation.

In [66], the authors propose a method to estimate the flexibility ranges at the boundary nodes between the distribution and transmission network. The resulting ranges show how much flexibility can be safely procured from a certain network node for a certain maximum price. This approach is different from the headroom concept explained above in the sense that the proposed flexibility ranges are calculated before the flexibility market takes place. The calculation also includes flexibility activation costs for the individual flexibility resources, which is not made available by the aggregators.

Here, we propose a computation method to calculate the available headroom capacity on a (distribution) network asset. The proposed method is inspired by the geometric approaches to represent (aggregated) flexibility as a convex polytope, allowing for a tractable calculation methodology.

4.2 Headroom: problem statement

4.2.1 Geometric characterization of flexibility

As explained in the introduction, it is reasonable to assume that there is a reporting duty of the maximal power of a flexible resource towards the DSO. The DSO is thus (only) aware of the location and maximum offtake (and/or injection) power of each flexible resource in the network.

The flexibility boundaries of the set of flexible resources N, connected to the same distribution feeder, can thus be represented as:

$$P_i^{min} \leq p_i \leq P_i^{max} \quad \forall i \in \{1, \cdots, N\} \tag{1}$$

with p_i the power offtake or injection from resource i at a specific timestep, and P_i^{min} and P_i^{max} the respective minimal and maximal power of the resource. Geometrically speaking, eq. (1) represents a hypercube in *N* dimensions, which is a particular type of convex polytope.

A (convex) polytope is a bounded polyhedron that can be always represented as $P := \{p \in R^N | Ap \leq b\}$, see for instance [67]. This is simply the feasible set of a set of linear constraints - provided it is bounded. So, the region delimited by the activation of these flexible resources can be described by the polytope:

$$\mathcal{P}_{flex} := \{p \in R^N | Ap \leq b\} \tag{2}$$

with

$$A = \begin{bmatrix} I \\ -I \end{bmatrix} \tag{3}$$

$$b = \begin{bmatrix} P^{max} \\ -P^{min} \end{bmatrix} \tag{4}$$

4.2.2 Geometric interpretation of distribution network constraints

The linearized 3-phase unbalanced power flow equations describing the voltages and currents on every node and through every branch of the distribution network can be expressed as a linear function of the net power offtake as follows:

$$v = Cp + c \tag{5}$$

$$i = Dp + d \tag{6}$$

with $v \in R^{3 \times m}$ and $i \in R^{3 \times (m-1)}$ the 3-phase voltage and current magnitude of the voltages and currents in a distribution network with m nodes, and $m-1$ branches. As distribution networks are generically operated radially, the number of branches equals the number of nodes-1 in such network.

Different methods are available in literature to obtain such linearization of the power flow equations, tailored for distribution networks. In [68], a fixed-point linearization method is introduced, resulting in sufficient accuracy of the voltage and current values. Other linearization of the power flow equations, such as e.g. the Taylor expansion as used in [69] also results in similar equations.

Here, matrices C and D, and vectors c and d are system parameters, that depend on the network. Also, the power offtake and injection from the uncontrollable load and generation, i.e. the operating point of the network, is included in these system parameters. An explanation on how to define these parameters can be found in the respective publications, e.g. [68]–[70].

Eq. (7) and (8) express the voltage and current limitations on the nodes and branches in the network and indicate the boundaries that must be respected when flexibility resources are activated.

$$\underline{v} \leq v \leq \overline{v} \tag{7}$$

$$\underline{i} \leq i \leq \overline{i} \tag{8}$$

Eq. (5)-(8) also form a convex polytope, $\mathcal{P}_{grid}$, that indicates the feasible region of flexible power activation on the distribution grid:

$$\mathcal{P}_{grid} := \{p \in R^N | Gp \leq g\} \tag{9}$$

with

$$G = \begin{bmatrix} C \\ -C \\ D \\ -D \end{bmatrix} \tag{10}$$

$$g = \begin{bmatrix} \overline{v} - c \\ -\underline{v} + c \\ \overline{i} - d \\ -\underline{i} + d \end{bmatrix} \tag{11}$$

The size of G equals $(12m - 6) \times N$, which for larger feeders may lead to a large size of G. However, some of the constraints described by the rows in G and g may be redundant and not binding.

It has been shown in the 70's already that eliminating redundant inequalities in a linear model is LP-equivalent [71]. The size of $\mathcal{P}_{grid}$ can thus often be reduced within polynomial time, leading to faster headroom calculations.

4.2.3 Headroom definition

As explained in the introduction, the headroom capacity of a feeder (or a substation) is defined as the maximal non-discriminating capacity available for flexibility activations. Positive flexibility corresponds to load increase. Negative flexibility corresponds to a load decrease, and in the case of batteries, injection is also possible. Both can step outside of $\mathcal{P}_{grid}$ because of current violations, eq. (8), over-voltage or under-voltage, eq. (7).

Based on these considerations, we define a region $\mathcal{H}$ as

$$\mathcal{H} = \{p \in R^N | \underline{\lambda} \leq \Lambda^T p \leq \overline{\lambda}\} \tag{12}$$

with $\Lambda \in R^N = [1,1,\cdots,1]$, and parameters $\underline{\lambda}$ and $\overline{\lambda}$ defined as the total minimum and maximum allowed flexibility in the network, they are thus the *headroom values for negative and positive flexibility* respectively.

The feasible region of flexibility can then be defined as the intersection of $\mathcal{H}$ with $\mathcal{P}_{flex}$:

$$\mathcal{P}'_{flex}(\overline{\lambda}, \underline{\lambda}) = \mathcal{H} \cap \mathcal{P}_{flex} \tag{13}$$

$$= \{p \in R^N | A'p \leq b' + \lambda\} \tag{14}$$

with

$$A' = \begin{bmatrix} A \\ \Lambda^T \\ -\Lambda^T \end{bmatrix} \tag{15}$$

$$b' = \begin{bmatrix} b \\ 0 \\ 0 \end{bmatrix} \tag{16}$$

$$\lambda = \begin{bmatrix} 0 \\ \overline{\lambda} \\ -\underline{\lambda} \end{bmatrix} \tag{17}$$

4.3 Finding the maximal headroom: optimization methodology

The feasible set $\mathcal{P}'_{flex}(\overline{\lambda}, \underline{\lambda})$ is parameterized by the choice of $\overline{\lambda}$ and $\underline{\lambda}$.

Finding the maximal headroom for *positive flexibility* resorts to finding the maximal value of $\overline{\lambda}$ so that $\mathcal{P}'_{flex}(\overline{\lambda}, \underline{\lambda})$ fits into $\mathcal{P}_{grid}$. Similarly, finding the maximal headroom for *negative flexibility* is then equal to finding the minimal value of $\underline{\lambda}$ so that $\mathcal{P}'_{flex}(\overline{\lambda}, \underline{\lambda})$ fits into $\mathcal{P}_{grid}$.
For simplicity reasons, we first assume that there is no negative flexibility available in the network, and hence $\underline{\lambda} = 0$.
The optimization problem can then be written as:

$$\begin{gathered} Obj. \max \overline{\lambda} \\ s.t. \;\; \mathcal{P}'_{flex}(\overline{\lambda}, \underline{\lambda}) \subseteq \mathcal{P}_{grid} \\ 0 \leq \overline{\lambda} \leq \lambda_{max} \\ \underline{\lambda} = 0 \end{gathered}$$

with λ_{max} being the upper bound of the positive flexibility, i.e. the maximal available positive flexibility in the network.

As two-dimensional polytopes are straightforward to visualize, an illustration of the geometrical interpretation of finding the maximal headroom capacity for a fictitious case with 2 flexible resources is shown Figure 4-2. The combined flexibility of both resources is bounded by $\mathcal{P}_{flex}$. As can be noted, both resources can be activated to consume extra power between a certain minimal, here assumed to be equal to 0, and maximal value, resulting in a hypercube.

The flexibility activation should be bounded within the network limitations, represented by $\mathcal{P}_{grid}$. Figure 4-2 shows 3 possible regions $\mathcal{H}$ of the form (12), each with a different value of $\overline{\lambda}$, and with the same value of $\underline{\lambda}$=0. When $\overline{\lambda}$, and thus the headroom capacity for positive flexibility, is too large, flexibility activation would be possible outside of $\mathcal{P}_{grid}$. When $\overline{\lambda}$ is too small, the headroom capacity would block an unacceptably large amount of the flexibility on the network asset.

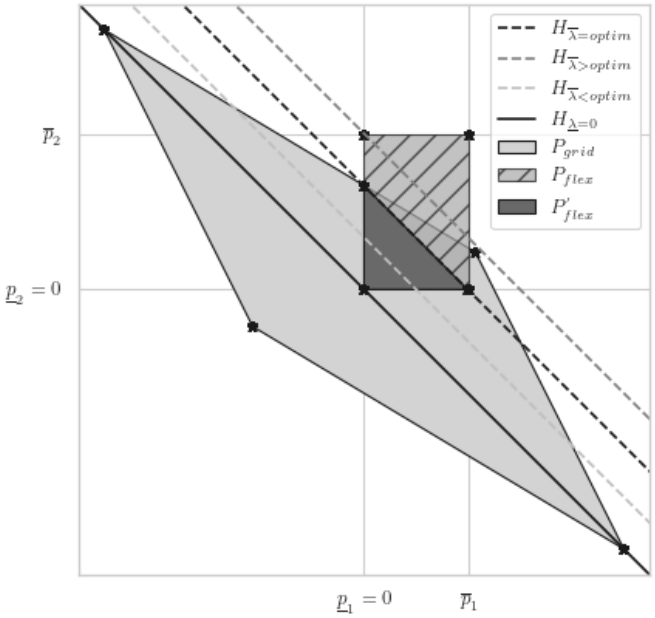

Figure 4-2: Geometrical interpretation of the maximal available capacity: the maximal allowed flexible capacity on a network segment is bounded by the region comprised between the lines $\mathcal{H}_{\underline{\lambda}=0}$ and $\mathcal{H}_{\overline{\lambda}=optim}$: there is no point within $\mathcal{P}'_{flex}$ outside of $\mathcal{P}_{grid}$. The regions bounded with $\mathcal{H}_{\overline{\lambda}<optim}$ and $\mathcal{H}_{\overline{\lambda}>optim}$ are also possible bounds on the flexibility activation, but these would lead to possible activation outside of $\mathcal{P}_{grid}$, or block a large amount of the available flexibility on the feeder.

To find the optimal value of $\bar{\lambda}$, and thus the maximal headroom capacity, an iterative optimization approach is proposed, outlined in Figure 4-3. Within each iteration, the value of $\bar{\lambda}$ is increased or decreased, and a check is done if the obtained $\mathcal{P}'_{flex}$ is fully contained in $\mathcal{P}_{grid}$. This is done by checking if for every row i of G and g, there is a point x contained by $\mathcal{P}'_{flex}$ where $G_i^T x - g_i > 0$. If this is the case, $\mathcal{P}'_{flex} \not\subseteq \mathcal{P}_{grid}$ and thus $\bar{\lambda}$ is set too high and must decrease. If on the other hand the obtained $\mathcal{P}'_{flex} \subseteq \mathcal{P}_{grid}$, $\bar{\lambda}$ might be too small, and may increase. This procedure is then repeated until a predefined accuracy ϵ is achieved.

Algorithm 1 Headroom calculation for positive flexibility

$\overline{\lambda}_{upp} \leftarrow \lambda_{max}$
$\overline{\lambda}_{low} \leftarrow 0$
$\Delta\lambda \leftarrow \overline{\lambda}_{upp} - \overline{\lambda}_{low}$
while $\Delta\lambda \geq \epsilon$ **do**
  $\overline{\lambda} \leftarrow \overline{\lambda}_{upp}$
  for i = 1 to number of rows in G **do**
    Solve the optimisation problem:
      Obj. $\max G_i^T x - g_i$
      s.t. $A' x \leq b' + \overline{\lambda} e$
    if Objective > 0 **then**
      $\overline{\lambda}_{upp} \leftarrow \overline{\lambda}_{low} + (\overline{\lambda}_{upp} - \overline{\lambda}_{low})/2$
      $\Delta\lambda \leftarrow \overline{\lambda}_{upp} - \overline{\lambda}_{low}$
      break
    end if
  end for
  if no positive objectives found **then**
    $\overline{\lambda}_{low} \leftarrow \overline{\lambda}$
    $\overline{\lambda}_{upp} \leftarrow \overline{\lambda}_{low} + (\overline{\lambda}_{upp} - \overline{\lambda}_{low})/2$
    $\Delta\lambda \leftarrow \overline{\lambda}_{upp} - \overline{\lambda}_{low}$
  end if
end while

Figure 4-3: Proposed calculation algorithm to find the maximal headroom for positive flexibility. A similar algorithm can be laid out to find the maximal headroom for negative flexibility.

The complexity of the proposed algorithm depends mainly on the size of G, and thus on the size of the network. As mentioned before, often the size of G can be reduced by removing redundant inequalities. Nevertheless, since the inner optimization problem is linear, and these can be solved efficiently with many available optimizers, the overall solution times remains tractable.

4.4 Case study

To show the results of the optimal headroom calculation, a case study is presented using the European LV test feeder presented in Chapter 2. This feeder has 55 (non-flexible) loads connected to it.

For this case study, several additional loads have been installed to the feeder:

- 35 PV installations. The peak capacity of the installations is randomly chosen between 3 or 5 kWp. The PV installations are randomly installed over the network.

- 10 Electric Vehicles, with a charging power of 3.7 kW. The EVs are randomly assigned to the customers on the network. The vehicles are assumed to be flexible loads.
- 18 Batteries, with a maximum power randomly chosen between 2, 2.5, 3 or 3.5 kW. Batteries are randomly assigned to the customers with a PV installation. The batteries are assumed to be flexible loads.

The maximal available positive flexibility is 81.5 kW, and maximal available negative flexibility is -44.5 kW.

The headroom capacity is calculated for a summer day. The energy offtake from the individual loads is modeled using the profiles available from the EU LV test feeder documentation. The PV production is assumed to follow an irradiance profile from an average summer day in Belgium. The baseline offtake from the EVs and batteries is assumed to be zero.

The voltage profile during the day of the furthest bus in the network, i.e. bus 114, is shown in Figure 4-4. To calculate the maximal headroom capacity on the network, voltage limits of +/- 0.05 p.u. are assumed, these limits are also indicated in Figure 4-4.

Figure 4-5 shows the resulting headroom capacity for positive and for negative flexibility on the network. The results show that positive flexibility must be limited during the evening and during the night: not all EVs and batteries can charge simultaneously at maximum power during the night. During the day however, when there is plenty of solar power available, no grid congestions will occur when all available positive flexibility is used.

Conversely, the maximal headroom capacity for negative flexibility is at its maximum during the night and during the evening but is limited during the day. This means that batteries can inject during the night and evening but can only inject limited power during the day.

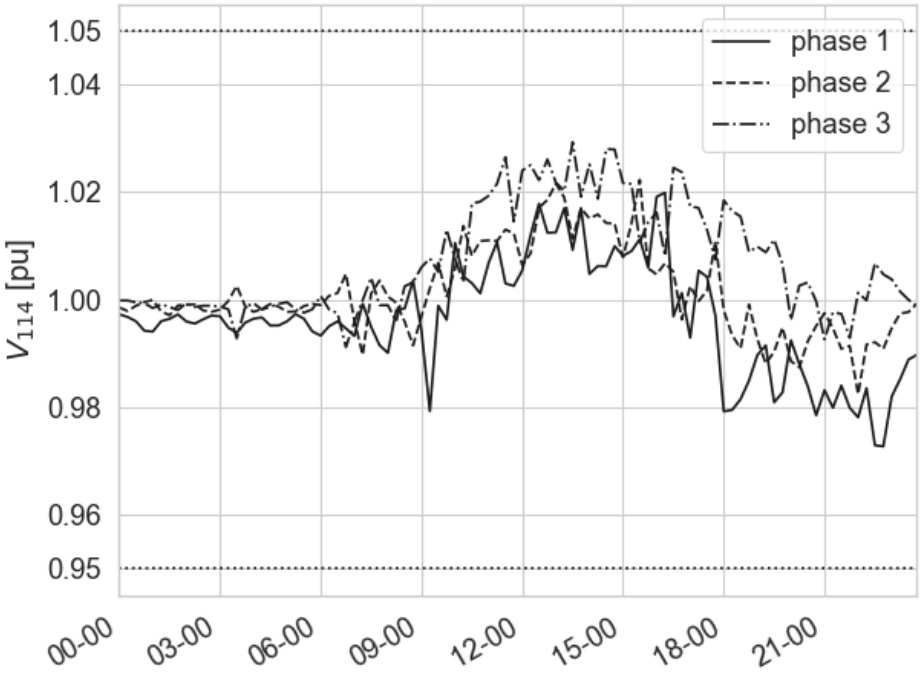

Figure 4-4: Baseline voltage of the voltage on the furthest bus in the network, i.e. bus 114. The voltage profile on the three phases is shown, as well as the voltage limits taken into account to determine the headroom capacities.

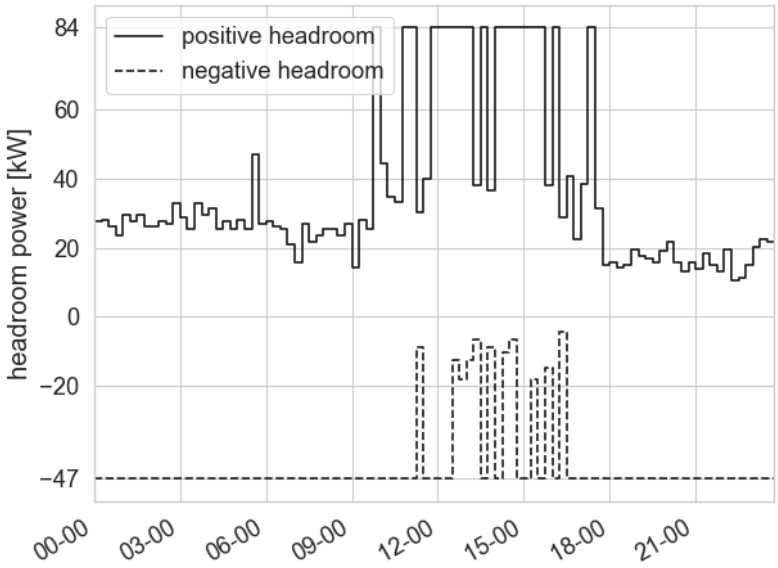

Figure 4-5: Maximal headroom capacity for positive flexibility (i.e. positive headroom), and for negative flexibility (i.e. negative headroom) for the case study.

Chapter 5 Conclusion

A sharp increase of low voltage (LV) demand flexibility is expected in the coming years. This is driven by the uptake of smart meters, roof top photovoltaic systems, home batteries, electric mobility and heat pumps. This large potential for flexibility in LV networks is primarily theoretical and it is to be unlocked. Hence, the main goal of this first deliverable (of WP3) is to present a solution that contributes to the unlock of LV flexibility.

Safe activation of LV flexibility without compromising network stability is one of the major issues that would prevent the full potential of LV flexibility. To safely activate LV flexibility, grid constraints need to be calculated. If grid constraints become visible, grid operators may communicate and coordinate with the flexibility providers and flexibility markets to avoid grid congestion.

Grid operators need a congestion forecaster to compute grid constraints. A congestion forecaster allows grid operators to identify where and when congestions will occur in the LV grid in case of activation of flexibility for system services, and provide spatially linked information on the risk for grid congestions to the stakeholders involved in providing system services.

Chapter 2 of this deliverable presents the LV congestion forecaster designed to identify the risk for congestion in LV networks under flexibility activation. The forecaster is based on statistical power flow. Chapter 3 of this deliverable presents the flexibility models of batteries providing frequency containment reserve (FCR), and the effect of FCR provided by LV flexibility on the congestion of the grid. Chapter 4 presents a novel method that calculates the available headroom capacity. The proposed method is inspired by the geometric approaches to represent aggregated flexibility as a convex polytope. The method of Chapter 4 enables the calculation of grid constraints, that in turn can be included in the adequacy and balancing mechanisms.

The IEEE European Low Voltage Test Feeder is used in this deliverable to study the different proposed implementations. The results show the ability of the LV congestion forecaster to calculate risk of congestion and grid constraints that would help DSOs avoid congestion.

References

[1] IRENA, "Future of Photovoltaic." https://www.irena.org/publications/2019/Nov/Future-of-Solar-Photovoltaic (accessed Dec. 08, 2022).

[2] M. Nijhuis, M. Gibescu, and J. F. G. Cobben, "Assessment of the impacts of the renewable energy and ICT driven energy transition on distribution networks," *Renewable and Sustainable Energy Reviews*, vol. 52, pp. 1003–1014, Dec. 2015, doi: 10.1016/j.rser.2015.07.124.

[3] ENTSO-E, "Review of Flexibility Platforms." https://www.entsoe.eu/news/2021/11/10/entso-e-publishes-new-report-on-flexibility-platforms/ (accessed Dec. 08, 2022).

[4] "dsoobservatory2018.pdf." Accessed: Sep. 29, 2022. [Online]. Available: https://ses.jrc.ec.europa.eu/sites/ses.jrc.ec.europa.eu/files/publications/dsoobservatory2018.pdf

[5] A. Srivastava *et al.*, "Development of a DSO support tool for congestion forecast," *IET Generation, Transmission & Distribution*, vol. 15, no. 23, pp. 3345–3359, 2021, doi: 10.1049/gtd2.12266.

[6] "Network Manager ADMS | Hitachi Energy." https://www.hitachienergy.com/offering/product-and-system/scada/network-management/network-manager-adms (accessed Sep. 29, 2022).

[7] "Spectrum Power Advanced Distribution Management," *siemens.com Global Website*. https://new.siemens.com/global/en/products/energy/energy-automation-and-smart-grid/grid-control/advanced-distribution-management.html (accessed Sep. 29, 2022).

[8] "ADMS (Advanced Distribution Management System)." https://www.se.com/ww/en/work/solutions/for-business/electric-utilities/advanced-distribution-management-system-adms/ (accessed Sep. 29, 2022).

[9] A. Srivastava, D. Steen, L. A. Tuan, and O. Carlson, "A Congestion Forecast Framework for Distribution Systems with High Penetration of PVs and PEVs," in *2019 IEEE Milan PowerTech*, Jun. 2019, pp. 1–6. doi: 10.1109/PTC.2019.8810871.

[10] S. Meinecke, L. Thurner, and M. Braun, "Review of Steady-State Electric Power Distribution System Datasets," *Energies*, vol. 13, no. 18, Art. no. 18, Jan. 2020, doi: 10.3390/en13184826.

[11] T. Hong, P. Pinson, Y. Wang, R. Weron, D. Yang, and H. Zareipour, "Energy Forecasting: A Review and Outlook," *IEEE Open Access Journal of Power and Energy*, vol. 7, pp. 376–388, 2020, doi: 10.1109/OAJPE.2020.3029979.

[12] S. Haben, S. Arora, G. Giasemidis, M. Voss, and D. Vukadinović Greetham, "Review of low voltage load forecasting: Methods, applications, and recommendations," *Applied Energy*, vol. 304, p. 117798, Dec. 2021, doi: 10.1016/j.apenergy.2021.117798.

[13] "Review of Smart Meter Data Analytics: Applications, Methodologies, and Challenges." https://ieeexplore.ieee.org/abstract/document/8322199/ (accessed Sep. 19, 2022).

[14] T. Gneiting and M. Katzfuss, "Probabilistic Forecasting." Rochester, NY, Jan. 01, 2014. doi: 10.1146/annurev-statistics-062713-085831.

[15] P. Chen, Z. Chen, and B. Bak-Jensen, "Probabilistic load flow: A review," in *2008 Third International Conference on Electric Utility Deregulation and Restructuring and Power Technologies*, Apr. 2008, pp. 1586–1591. doi: 10.1109/DRPT.2008.4523658.

[16] T. Hong and S. Fan, "Probabilistic electric load forecasting: A tutorial review," *International Journal of Forecasting*, vol. 32, no. 3, Art. no. 3, Jul. 2016, doi: 10.1016/j.ijforecast.2015.11.011.

[17] B. Yildiz, J. I. Bilbao, J. Dore, and A. B. Sproul, "Recent advances in the analysis of residential electricity consumption and applications of smart meter data," *Applied Energy*, vol. 208, pp. 402–427, Dec. 2017, doi: 10.1016/j.apenergy.2017.10.014.

[18] M. S. Srinivas, "Distribution load flows: a brief review," in *2000 IEEE Power Engineering Society Winter Meeting. Conference Proceedings (Cat. No.00CH37077)*, Jan. 2000, vol. 2, pp. 942–945 vol.2. doi: 10.1109/PESW.2000.850058.

[19] R. Berg, E. S. Hawkins, and W. W. Pleines, "Mechanized Calculation of Unbalanced Load Flow on Radial Distribution Circuits," *IEEE Transactions on Power Apparatus and Systems*, vol. PAS-86, no. 4, pp. 415–421, Apr. 1967, doi: 10.1109/TPAS.1967.291849.

[20] *Commission Regulation (EU) 2015/1222 of 24 July 2015 establishing a guideline on capacity allocation and congestion management (Text with EEA relevance)*, vol. 197. 2015. Accessed: Sep. 29, 2022. [Online]. Available: http://data.europa.eu/eli/reg/2015/1222/oj/eng
[21] *Regulation (EU) 2019/943 of the European Parliament and of the Council of 5 June 2019 on the internal market for electricity (recast) (Text with EEA relevance.)*, vol. 158. 2019. Accessed: Sep. 29, 2022. [Online]. Available: http://data.europa.eu/eli/reg/2019/943/oj/eng
[22] "Resources – IEEE PES Test Feeder." https://cmte.ieee.org/pes-testfeeders/resources/ (accessed Dec. 07, 2022).
[23] M. A. Khan and B. P. Hayes, "A Reduced Electrically-Equivalent Model of the IEEE European Low Voltage Test Feeder," in *2022 IEEE Power & Energy Society General Meeting (PESGM)*, Jul. 2022, pp. 1–5. doi: 10.1109/PESGM48719.2022.9916806.
[24] HJ, "Renewable energy targets," *Energy - European Commission*, Jul. 08, 2021. https://ec.europa.eu/energy/topics/renewable-energy/directive-targets-and-rules/renewable-energy-targets_en (accessed Oct. 21, 2021).
[25] "Renewable Energy Sources and Climate Change Mitigation — IPCC." https://www.ipcc.ch/report/renewable-energy-sources-and-climate-change-mitigation/ (accessed Oct. 21, 2021).
[26] "Regulation (EU) 2017/1485." https://lexparency.org/eu/32017R1485/ (accessed Dec. 12, 2022).
[27] "DIRECTIVE (EU) 2019/ 944 OF THE EUROPEAN PARLIAMENT AND OF THE COUNCIL - of 5 June 2019 - on common rules for the internal market for electricity and amending Directive 2012/ 27/ EU," p. 75.
[28] "210722_TSO-DSO-Task-Force-on-Distributed-Flexibility_proofread-FINAL-2.pdf." Accessed: Jan. 13, 2022. [Online]. Available: https://www.edsoforsmartgrids.eu/wp-content/uploads/210722_TSO-DSO-Task-Force-on-Distributed-Flexibility_proofread-FINAL-2.pdf
[29] "20200603-GEODE-PP-SECTOR-INTEGRATION.pdf." Accessed: Jan. 18, 2022. [Online]. Available: https://www.geode-eu.org/wp-content/uploads/2020/06/20200603-GEODE-PP-SECTOR-INTEGRATION.pdf
[30] "Flexibility-in-the-energy-transition-A-tool-for-electricity-DSOs-2018-HD.pdf." Accessed: Jan. 13, 2022. [Online]. Available: https://www.edsoforsmartgrids.eu/wp-content/uploads/Flexibility-in-the-energy-transition-A-tool-for-electricity-DSOs-2018-HD.pdf
[31] "recommendations-on-the-use-of-flexibility-in-distribution-networks_proof-h-86B1B173.pdf." Accessed: Feb. 04, 2022. [Online]. Available: https://www.eurelectric.org/media/4410/recommendations-on-the-use-of-flexibility-in-distribution-networks_proof-h-86B1B173.pdf
[32] "entsoe_TSO-DSO_DMR_web.pdf." Accessed: Feb. 03, 2022. [Online]. Available: https://eepublicdownloads.entsoe.eu/clean-documents/Publications/Position%20papers%20and%20reports/entsoe_TSO-DSO_DMR_web.pdf
[33] M. Zidar, P. S. Georgilakis, N. D. Hatziargyriou, T. Capuder, and D. Škrlec, "Review of energy storage allocation in power distribution networks: applications, methods and future research," *IET Generation, Transmission & Distribution*, vol. 10, no. 3, pp. 645–652, 2016, doi: 10.1049/iet-gtd.2015.0447.
[34] N. Karthikeyan, B. R. Pokhrel, J. R. Pillai, and B. Bak-Jensen, "Utilization of Battery Storage for Flexible Power Management in Active Distribution Networks," in *2018 IEEE Power & Energy Society General Meeting (PESGM)*, Aug. 2018, pp. 1–5. doi: 10.1109/PESGM.2018.8586215.
[35] F. Marra, G. Yang, C. Træholt, J. Østergaard, and E. Larsen, "A Decentralized Storage Strategy for Residential Feeders With Photovoltaics," *IEEE Transactions on Smart Grid*, vol. 5, no. 2, pp. 974–981, Mar. 2014, doi: 10.1109/TSG.2013.2281175.
[36] P. Fortenbacher, J. L. Mathieu, and G. Andersson, "Modeling and Optimal Operation of Distributed Battery Storage in Low Voltage Grids," *IEEE Transactions on Power Systems*, vol. 32, no. 6, pp. 4340–4350, Nov. 2017, doi: 10.1109/TPWRS.2017.2682339.
[37] M. Brandao, H. Johal, and L. Ion, "Energy storage for LV grid support in Australia," in *2011 IEEE PES Innovative Smart Grid Technologies*, Nov. 2011, pp. 1–8. doi: 10.1109/ISGT-Asia.2011.6167103.

[38] J. Engels, B. Claessens, and G. Deconinck, "Combined Stochastic Optimization of Frequency Control and Self-Consumption With a Battery," *IEEE Transactions on Smart Grid*, vol. 10, no. 2, pp. 1971–1981, Mar. 2019, doi: 10.1109/TSG.2017.2785040.
[39] G. B. M. A. Litjens, E. Worrell, and W. G. J. H. M. van Sark, "Economic benefits of combining self-consumption enhancement with frequency restoration reserves provision by photovoltaic-battery systems," *Applied Energy*, vol. 223, pp. 172–187, Aug. 2018, doi: 10.1016/j.apenergy.2018.04.018.
[40] J. Engels, B. Claessens, and G. Deconinck, "Grid-Constrained Distributed Optimization for Frequency Control With Low-Voltage Flexibility," *IEEE Transactions on Smart Grid*, vol. 11, no. 1, pp. 612–622, Jan. 2020, doi: 10.1109/TSG.2019.2926956.
[41] M. Roos and B. Holthuizen, "Congestion of LV Distribution Networks by Household Battery Energy Storage Systems utilized for FCR, aFRR and Market Trading," in *2018 53rd International Universities Power Engineering Conference (UPEC)*, Sep. 2018, pp. 1–6. doi: 10.1109/UPEC.2018.8541879.
[42] A. Shahsavari *et al.*, "Distribution Grid Reliability Versus Regulation Market Efficiency: An Analysis Based on Micro-PMU Data," *IEEE Transactions on Smart Grid*, vol. 8, no. 6, pp. 2916–2925, Nov. 2017, doi: 10.1109/TSG.2017.2718560.
[43] "Regulation (EC) No 714/2009 of the European Parliament and of the Council of 13 July 2009 on conditions for access to the network for cross-border exchanges in electricity and repealing Regulation (EC) No 1228/2003," p. 21.
[44] Elia, "FCR service design note - Market development (April 2019)." 2019.
[45] Skill-Lync, "Mathematical Model of a Battery," *Skill-Lync*, Jul. 05, 2022. https://skill-lync.com/student-projects/mathematical-model-of-a-battery-2 (accessed Jul. 05, 2022).
[46] Y. Yu *et al.*, "Constructing Accurate Equivalent Electrical Circuit Models of Lithium Iron Phosphate and Lead–Acid Battery Cells for Solar Home System Applications," *Energies*, vol. 11, no. 9, Art. no. 9, Sep. 2018, doi: 10.3390/en11092305.
[47] S. Tamilselvi *et al.*, "A Review on Battery Modelling Techniques," *Sustainability*, vol. 13, no. 18, Art. no. 18, Jan. 2021, doi: 10.3390/su131810042.
[48] S. Ruggeri, G. Celli, F. Pilo, G. Malarange, and A. Pagnetti, "Simplified LV feeders model in presence of DG for MV network studies," *Sustainable Energy, Grids and Networks*, vol. 13, pp. 19–28, Mar. 2018, doi: 10.1016/j.segan.2017.10.002.
[49] IRENA, "World energy transitions outlook: 1.5°C pathway." 2022.
[50] The European Parliament, "Directive (EU) 2019/944 of the European Parliament and of the council of 5 June 2019 on common rules for the internal market for electricity and amending directive 2012/27/EU." 2019.
[51] Council of European Energy Regulator's (CEER), "CEER 2022-2025 strategy empowering consumers for the energy transition." 2021.
[52] Synergrid, "C8-01 Network Flexibility Study voor de deelname van de DNG's aan flexibiliteitsdiensten. (in Dutch)." 2021.
[53] S. Bashash and H. K. Fathy, "Modeling and Control of Aggregate Air Conditioning Loads for Robust Renewable Power Management," *IEEE Transactions on Control Systems Technology*, vol. 21, no. 4, pp. 1318–1327, Jul. 2013, doi: 10.1109/TCST.2012.2204261.
[54] L. Zhao, W. Zhang, H. Hao, and K. Kalsi, "A Geometric Approach to Aggregate Flexibility Modeling of Thermostatically Controlled Loads," *IEEE Transactions on Power Systems*, vol. 32, no. 6, pp. 4721–4731, Nov. 2017, doi: 10.1109/TPWRS.2017.2674699.
[55] S. Wang and W. Wu, "Aggregate Flexibility of Virtual Power Plants With Temporal Coupling Constraints," *IEEE Transactions on Smart Grid*, vol. 12, no. 6, pp. 5043–5051, Nov. 2021, doi: 10.1109/TSG.2021.3106646.
[56] Y. Wen, Z. Hu, S. You, and X. Duan, "Aggregate Feasible Region of DERs: Exact Formulation and Approximate Models," *IEEE Transactions on Smart Grid*, vol. 13, no. 6, pp. 4405–4423, Nov. 2022, doi: 10.1109/TSG.2022.3179998.
[57] V. Trovato, S. H. Tindemans, and G. Strbac, "Leaky storage model for optimal multi-service allocation of thermostatic loads," *IET Generation, Transmission & Distribution*, vol. 10, no. 3, pp. 585–593, 2016, doi: 10.1049/iet-gtd.2015.0168.

[58] G. D. Zotti, S. A. Pourmousavi, J. M. Morales, H. Madsen, and N. K. Poulsen, "A Control-Based Method to Meet TSO and DSO Ancillary Services Needs by Flexible End-Users," *IEEE Transactions on Power Systems*, vol. 35, no. 3, pp. 1868–1880, May 2020, doi: 10.1109/TPWRS.2019.2951623.

[59] S. Barot and J. A. Taylor, "A concise, approximate representation of a collection of loads described by polytopes," *International Journal of Electrical Power & Energy Systems*, vol. 84, pp. 55–63, Jan. 2017, doi: 10.1016/j.ijepes.2016.05.001.

[60] F. L. Müller, J. Szabó, O. Sundström, and J. Lygeros, "Aggregation and Disaggregation of Energetic Flexibility From Distributed Energy Resources," *IEEE Transactions on Smart Grid*, vol. 10, no. 2, pp. 1205–1214, Mar. 2019, doi: 10.1109/TSG.2017.2761439.

[61] K. Trangbaek and J. Bendtsen, "Exact constraint aggregation with applications to smart grids and resource distribution," in *2012 IEEE 51st IEEE Conference on Decision and Control (CDC)*, Dec. 2012, pp. 4181–4186. doi: 10.1109/CDC.2012.6426475.

[62] B. Cui, A. Zamzam, and A. Bernstein, "Network-Cognizant Time-Coupled Aggregate Flexibility of Distribution Systems Under Uncertainties," in *2021 American Control Conference (ACC)*, May 2021, pp. 4178–4183. doi: 10.23919/ACC50511.2021.9482808.

[63] M. U. Hashmi, A. Koirala, H. Ergun, and D. Van Hertem, "Flexible and curtailable resource activation in a distribution network using nodal sensitivities," in *2021 International Conference on Smart Energy Systems and Technologies (SEST)*, Sep. 2021, pp. 1–6. doi: 10.1109/SEST50973.2021.9543215.

[64] X. Chen, E. Dall'Anese, C. Zhao, and N. Li, "Aggregate Power Flexibility in Unbalanced Distribution Systems," *IEEE Transactions on Smart Grid*, vol. 11, no. 1, pp. 258–269, Jan. 2020, doi: 10.1109/TSG.2019.2920991.

[65] X. Chen and N. Li, "Leveraging Two-Stage Adaptive Robust Optimization for Power Flexibility Aggregation," *IEEE Transactions on Smart Grid*, vol. 12, no. 5, pp. 3954–3965, Sep. 2021, doi: 10.1109/TSG.2021.3068341.

[66] J. Silva *et al.*, "Estimating the Active and Reactive Power Flexibility Area at the TSO-DSO Interface," *IEEE Transactions on Power Systems*, vol. 33, no. 5, pp. 4741–4750, Sep. 2018, doi: 10.1109/TPWRS.2018.2805765.

[67] G. M. Ziegler and G. M. Ziegler, *Lectures on Polytopes*. Springer New York, 1995.

[68] A. Bernstein, C. Wang, E. Dall'Anese, J.-Y. Le Boudec, and C. Zhao, "Load Flow in Multiphase Distribution Networks: Existence, Uniqueness, Non-Singularity and Linear Models," *IEEE Transactions on Power Systems*, vol. 33, no. 6, pp. 5832–5843, Nov. 2018, doi: 10.1109/TPWRS.2018.2823277.

[69] K. Christakou, J.-Y. LeBoudec, M. Paolone, and D.-C. Tomozei, "Efficient Computation of Sensitivity Coefficients of Node Voltages and Line Currents in Unbalanced Radial Electrical Distribution Networks," *IEEE Transactions on Smart Grid*, vol. 4, no. 2, pp. 741–750, Jun. 2013, doi: 10.1109/TSG.2012.2221751.

[70] A. Bernstein and E. Dall'Anese, "Linear power-flow models in multiphase distribution networks," in *2017 IEEE PES Innovative Smart Grid Technologies Conference Europe (ISGT-Europe)*, Sep. 2017, pp. 1–6. doi: 10.1109/ISGTEurope.2017.8260205.

[71] J. Telgen, "ON REDUNDANCY IN SYSTEMS OF LINEAR INEQUALITIES," 2018. Accessed: Dec. 07, 2022. [Online]. Available: https://ageconsearch.umn.edu/record/272154/files/erasmus091.pdf